Structural and Rate Studies of the Formation and Trapping of Benzyne

Jason C. Riggs,[a] Antonio Ramirez,[a] Matthew E. Cremeens,[a] John Candler,[b] Crystal G. Bashore,[b] Michael C. Wirtz,[b] Jotham W. Coe,[b]* and David B. Collum[a]*

Contribution from the Department of Chemistry and Chemical Biology
[a]*Baker Laboratory, Cornell University, Ithaca, New York 14853-1301*
[b]*Pfizer Global Research and Development, Groton Laboratories, Pfizer, Inc., Groton, CT 06340*

Supporting Information

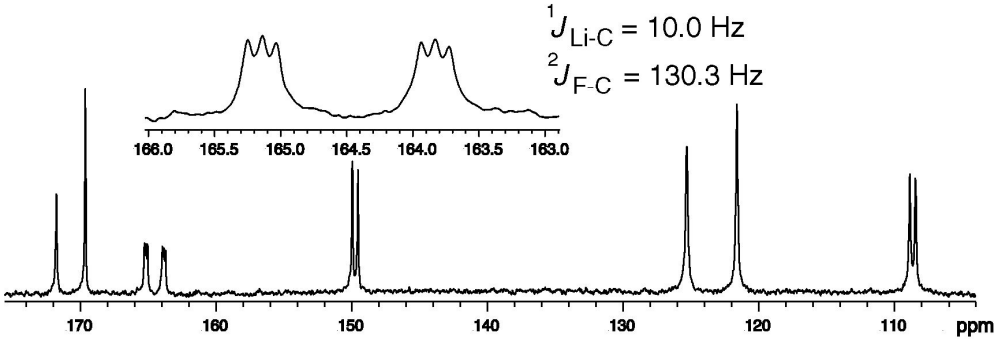

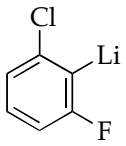

6

I. ^{13}C NMR spectrum in neat THF at –100 ˚C of 0.4 M [^{6}Li]2-chloro-6-fluorophenyllithium (**6**).

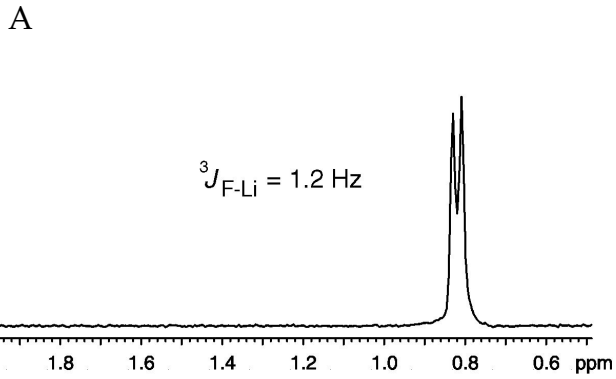

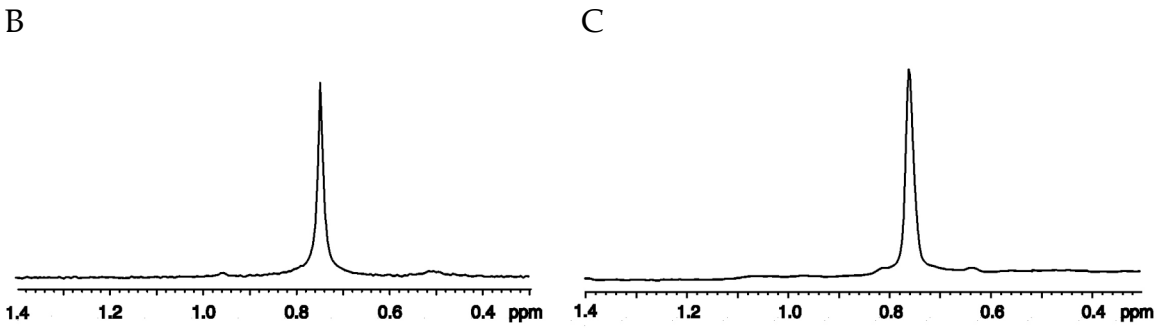

II. ^{6}Li NMR spectra in THF and pentane cosolvent of: (A) 0.20 M [^{6}Li]-**6** in 10.3 M THF at –100 ˚C; (B) 0.10 M [^{6}Li]-**6** in 5.0 M THF at –85 ˚C; (C) 0.10 M [^{6}Li]-**6** in 0.3 M THF at –85 ˚C.

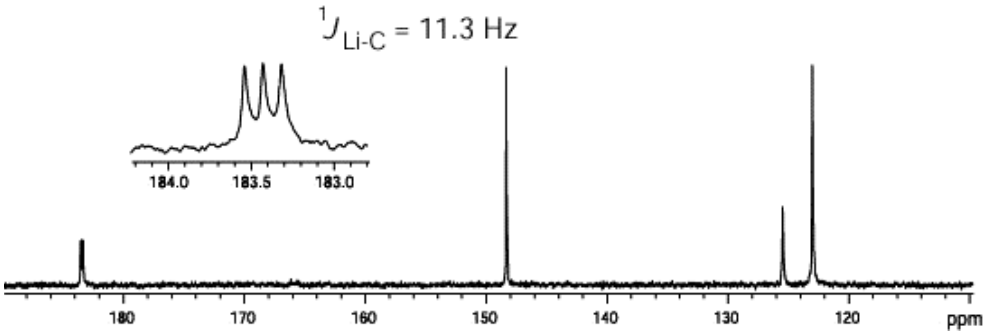

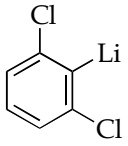

7

III. ^{13}C NMR spectrum in neat THF at –100 ˚C of 0.4 M [^{6}Li]2,6-dichlorophenyllithium (**7**).

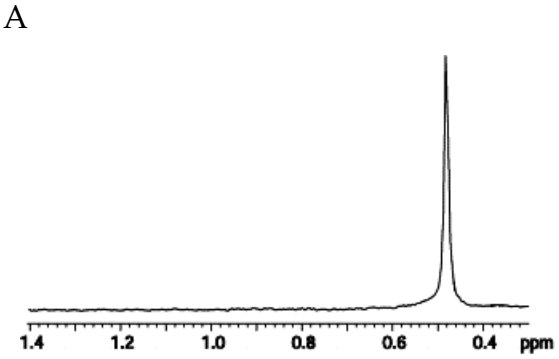

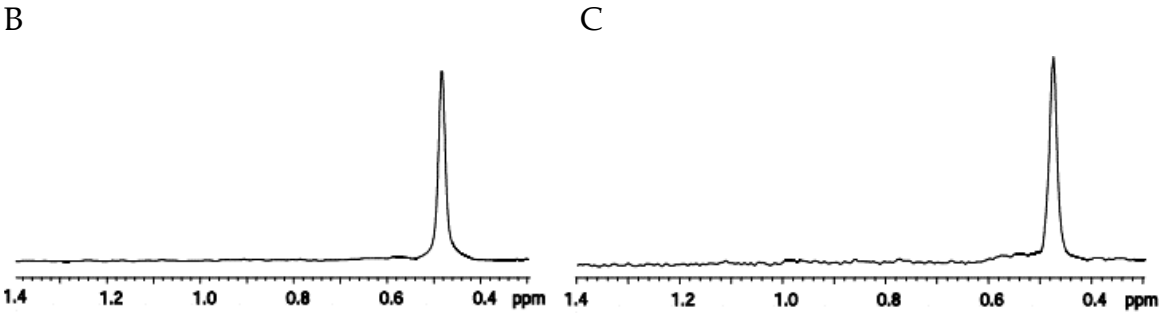

IV. ^{6}Li NMR spectra in THF and toluene cosolvent of: (A) 0.20 M [^{6}Li]-**7** in 10.3 M THF at –100 ˚C; (B) 0.10 M [^{6}Li]-**7** in 5.0 M THF at –85 ˚C; (C) 0.10 M [^{6}Li]-**7** in 0.3 M THF at –85 ˚C.

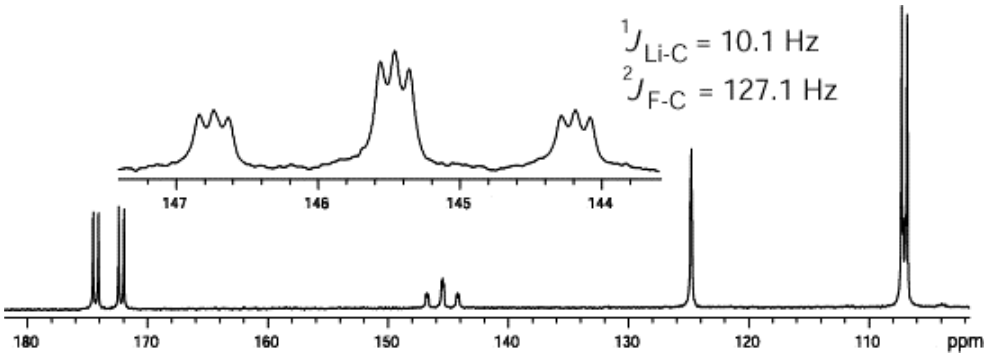

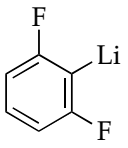

8

V. ^{13}C NMR spectrum in neat THF at –100 ˚C of 0.4 M [^{6}Li]2,6-difluorophenyllithium (**8**).

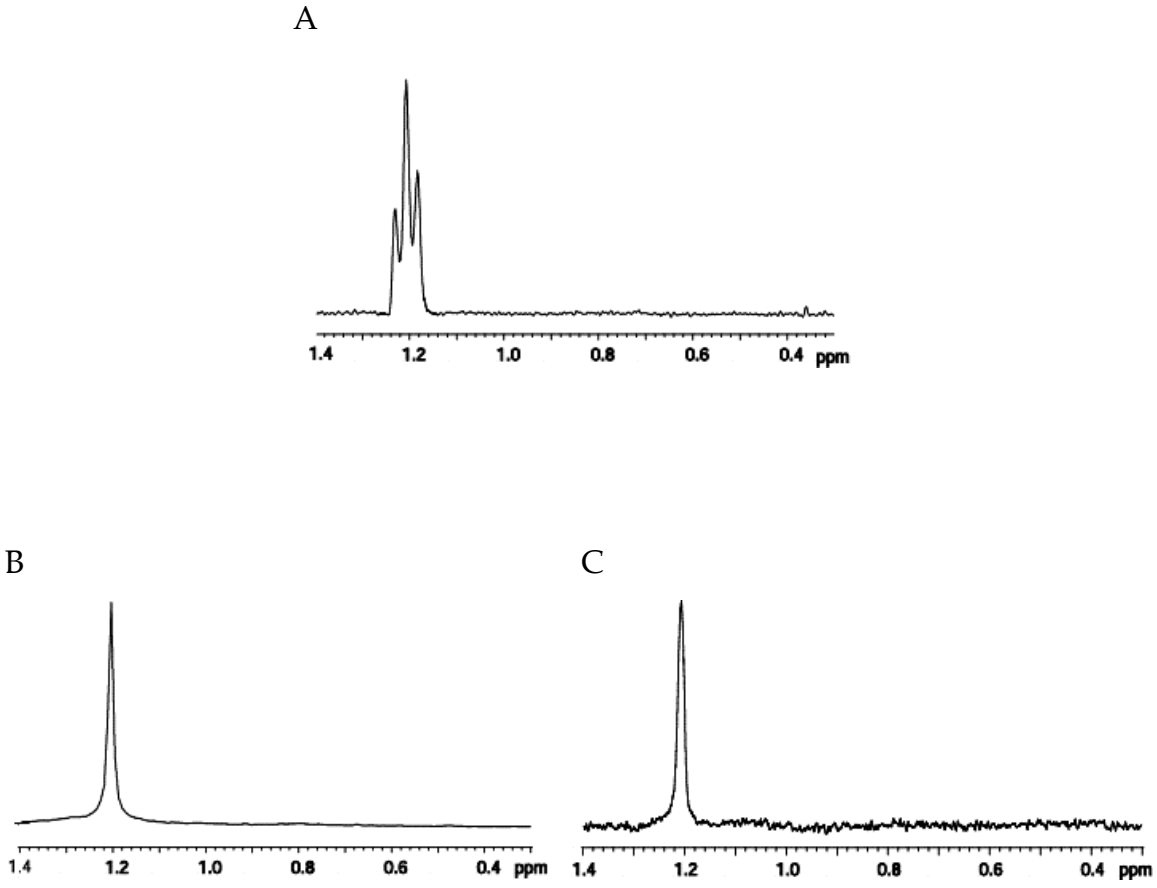

VI. ^{6}Li NMR spectra in THF and toluene cosolvent of: (A) 0.20 M [^{6}Li]-**8** in 10.3 M THF at –100 ˚C; (B) 0.10 M [^{6}Li]-**8** in 5.0 M THF at –85 ˚C; (C) 0.10 M [^{6}Li]-**8** in 0.3 M THF at –85 ˚C.

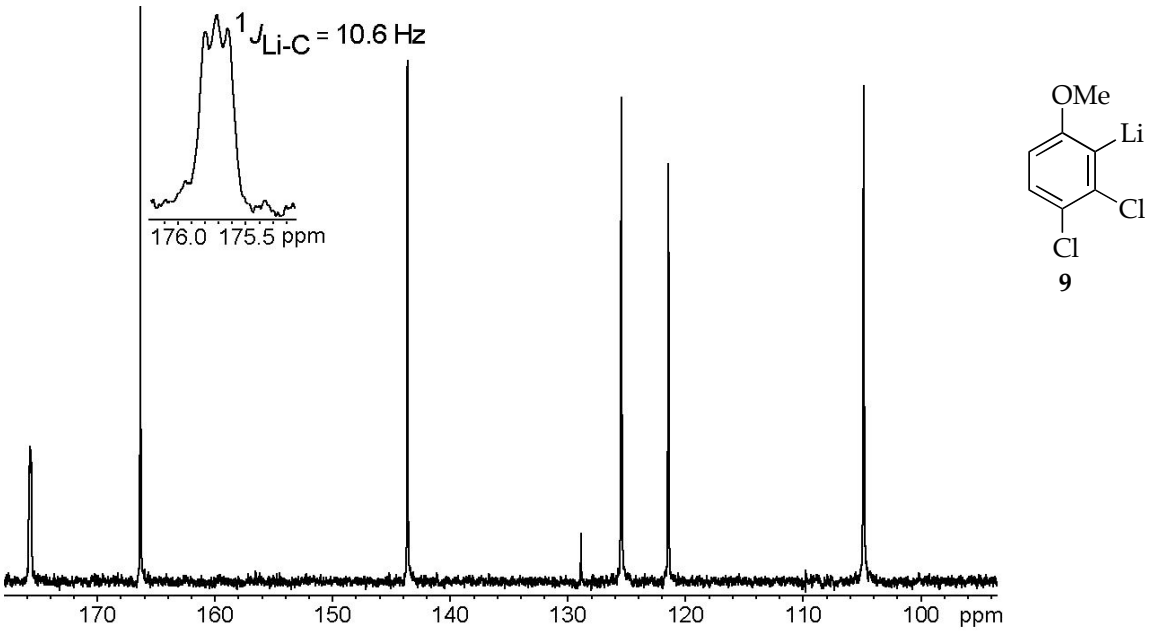

VII. ^{13}C NMR spectrum in 10.0 M THF and pentane co-solvent at –110 °C of 0.3 M [^{6}Li]2,3-dichloro-6-methoxyphenyllithium (**9**). *Me*O resonance at 54.2 ppm not shown.

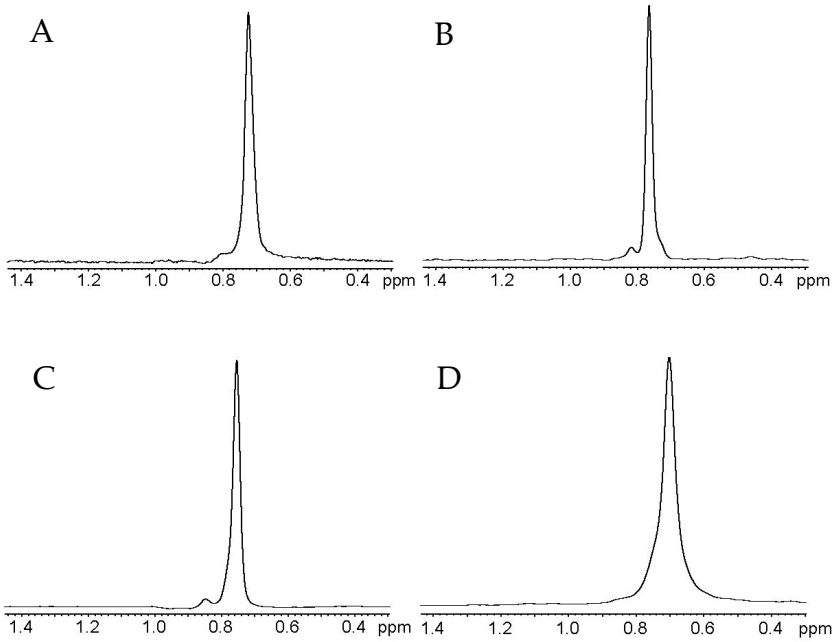

VIII. ^{6}Li NMR spectra in THF and toluene/pentane cosolvent of: (A) 0.10 M [^{6}Li]-**9** 5.0 M THF at – 80 °C; (B) 0.10 M [^{6}Li]-**9** in 10.0 M THF at – 80 °C; (C) 0.30 M [^{6}Li]-**9** in 5.0 M THF at – 80 °C; (D) 0.30 M [^{6}Li]-**9** in 5.0 M THF at – 110 °C.

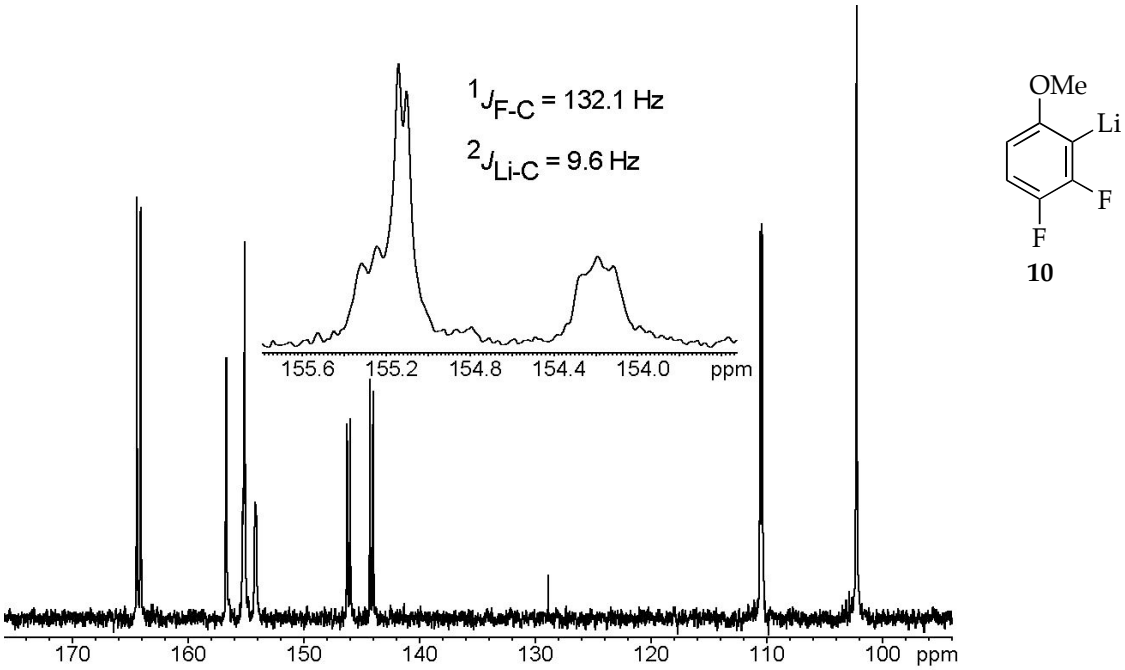

10

IX. ^{13}C NMR spectrum in 10.0 M THF and pentane co-solvent at –115 °C of 0.3 M [^{6}Li]2,3-difluoro-6-methoxyphenyllithium (**10**). *Me*O resonance at 54.1 ppm not shown.

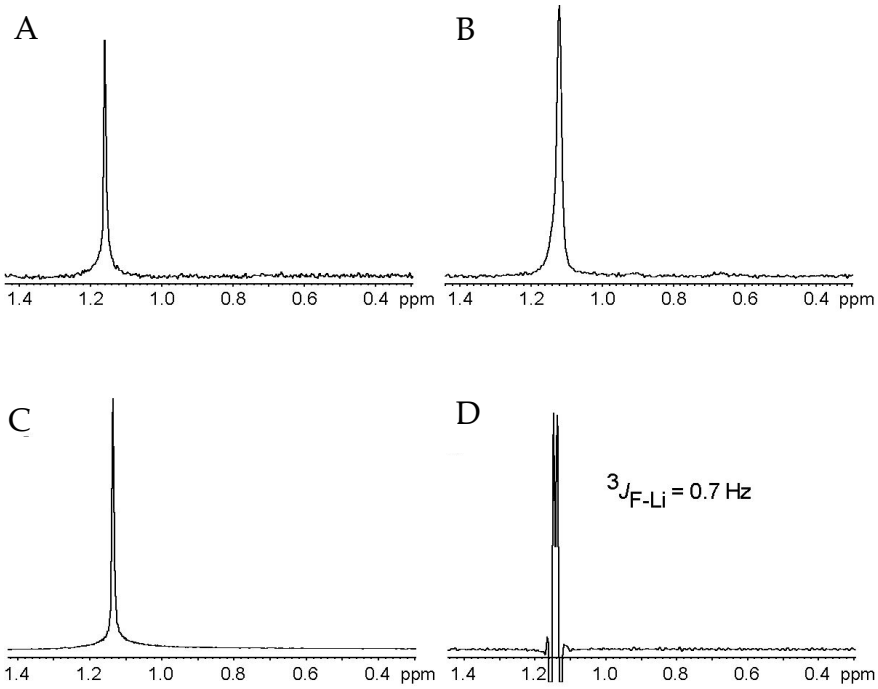

X. ^{6}Li NMR spectra in THF and toluene/pentane cosolvent of: (A) 0.10 M [^{6}Li]-**10** 5.0 M THF at – 90 °C; (B) 0.10 M [^{6}Li]-**10** in 10.0 M THF at – 90 °C; (C) 0.30 M [^{6}Li]-**10** in 5.0 M THF at – 90 °C; (D) 0.30 M [^{6}Li]-**9** in 5.0 M THF at – 110 °C.

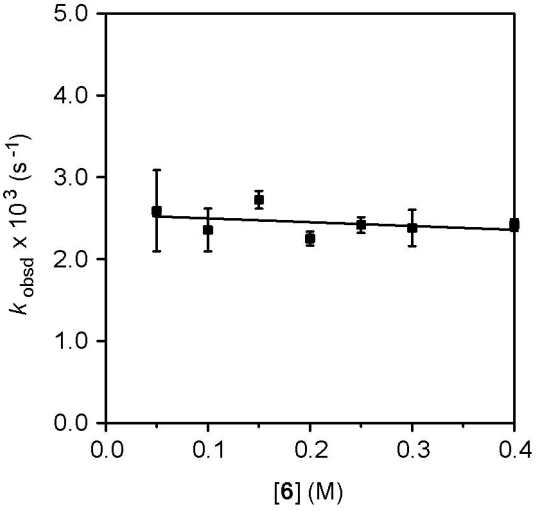

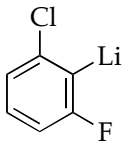

6

XI. Plot of $k_{obsd(6)}$ versus [**6**] in THF (0.3 M) and toluene cosolvent for the formation of 3-chloro- and 3-fluorobenzyne at -25 °C. The curve depicts the result of an unweighted least-squares fit to $k_{obsd} = k[\mathbf{6}] + k'$ ($k = 5 \pm 5 \times 10^{-4}$, $k' = 2.5 \pm 0.1 \times 10^{-3}$).

[**6**] (M)	$k_{obsd}1$ (s^{-1})	$k_{obsd}2$ (s^{-1})	k_{obsd}av (s^{-1})
0.050	0.0029 ± 3E-4	0.0022 ± 2E-4	0.0026 ± 5E-4
0.100	0.0022 ± 1E-4	0.0025 ± 2E-4	0.0023 ± 3E-4
0.150	0.0026 ± 1E-4	0.0028 ± 3E-4	0.0027 ± 1E-4
0.200	0.0022 ± 2E-4	0.0023 ± 2E-4	0.0022 ± 1E-4
0.250	0.0025 ± 3E-4	0.0023 ± 2E-4	0.0024 ± 1E-4
0.300	0.0025 ± 2E-4	0.0022 ± 2E-4	0.0024 ± 2E-4
0.400	0.0024 ± 2E-4	0.0025 ± 3E-4	0.0024 ± 1E-4

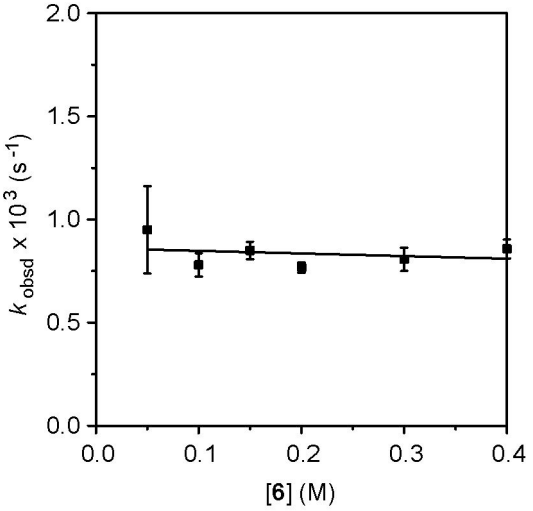

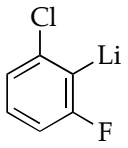

6

XII. Plot of k_{obsd} versus [**6**] in THF (6.8 M) and toluene cosolvent for the formation of 3-chloro- and 3-fluorobenzyne at -25 °C. The curve depicts the result of an unweighted least-squares fit to $k_{obsd} = k[\mathbf{6}] + k'$ ($k = 1 \pm 2 \times 10^{-4}$, $k' = 8.6 \pm 0.6 \times 10^{-4}$).

[**6**] (M)	$k_{obsd}1$ (s^{-1})	$k_{obsd}2$ (s^{-1})	k_{obsd}av (s^{-1})
0.050	0.0008 ± 1E-4	0.0011 ± 1E-4	0.0009 ± 2E-4
0.100	0.00082 ± 5E-5	0.00074 ± 3E-5	0.00078 ± 6E-5
0.150	0.00088 ± 4E-5	0.00082 ± 5E-5	0.00085 ± 4E-5
0.200	0.00075 ± 8E-5	0.00078 ± 5E-5	0.00077 ± 2E-5
0.300	0.0008 ± 1E-4	0.00077 ± 4E-5	0.00081 ± 5E-5
0.400	0.0008 ± 1E-4	0.00089 ± 1E-5	0.00086 ± 5E-5

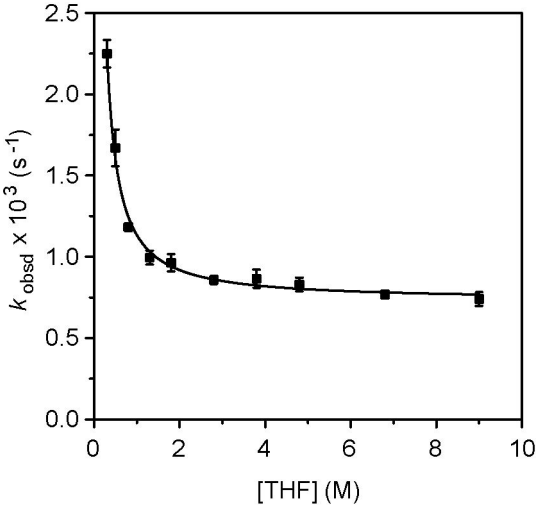

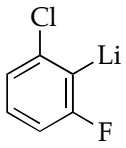

6

XIII. Plot of k_{obsd} versus [THF] in toluene cosolvent for the formation of 3-chloro- and 3-fluorobenzyne from **6** (0.2 M) at -25 °C. The curve depicts the result of an unweighted least-squares fit to $k_{obsd} = k[THF]^n + k'$ ($k = 4.0 \pm 0.4 \times 10^{-5}$, n = -1.12 $\pm$ 0.09, $k' = 7.3 \pm 0.3 \times 10^{-4}$).

[THF] (M)	$k_{obsd}1$ (s^{-1})	$k_{obsd}2$ (s^{-1})	k_{obsd}av (s^{-1})
0.30	0.0022 $\pm$ 2E-4	0.0023 $\pm$ 2E-4	0.0022 $\pm$ 1E-4
0.50	0.0017 $\pm$ 1E-4	0.0016 $\pm$ 2E-4	0.0017 $\pm$ 1E-4
0.80	0.0012 $\pm$ 1E-4	0.0012 $\pm$ 1E-4	0.0012 $\pm$ 1E-4
1.30	0.0010 $\pm$ 1E-4	0.00096 $\pm$ 8E-5	0.00099 $\pm$ 4E-5
1.80	0.00092 $\pm$ 5E-5	0.0010 $\pm$ 1E-4	0.00096 $\pm$ 5E-5
2.80	0.00087 $\pm$ 4E-5	0.00084 $\pm$ 5E-5	0.00086 $\pm$ 2E-5
3.80	0.00082 $\pm$ 4E-5	0.00090 $\pm$ 3E-5	0.00086 $\pm$ 6E-5
4.80	0.0009 $\pm$ 1E-4	0.00080 $\pm$ 5E-5	0.00083 $\pm$ 4E-5
6.80	0.00075 $\pm$ 8E-5	0.00078 $\pm$ 5E-5	0.00077 $\pm$ 2E-5
9.00	0.00071 $\pm$ 6E-5	0.00077 $\pm$ 8E-5	0.00074 $\pm$ 4E-5

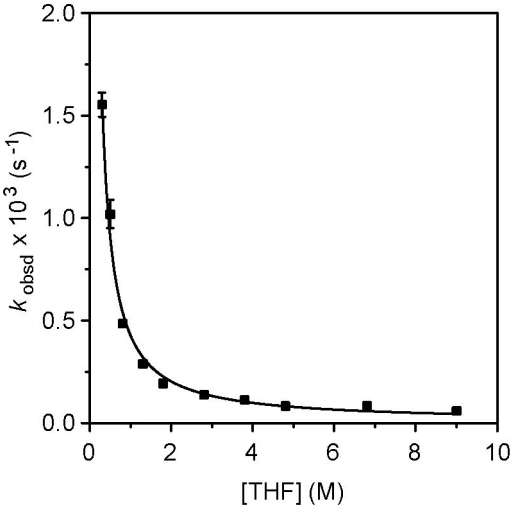

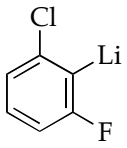

6

XIV. Plot of k_{obsd} versus [THF] in toluene cosolvent for the formation of 3-chlorobenzyne (**4a**) from **6** (0.2 M) at -25 °C. The curve depicts the result of an unweighted least-squares fit to $k_{obsd} = k[\text{THF}]^n + k'$ ($k = 4.2 \pm 0.6 \times 10^{-4}$, n = -1.1 $\pm$ 0.1, $k' = 1 \pm 4 \times 10^{-5}$).

[THF] (M)	$k_{obsd}1$ (s^{-1})	$k_{obsd}2$ (s^{-1})	k_{obsd}av (s^{-1})
0.30	0.0015 $\pm$ 1E-4	0.0016 $\pm$ 1E-4	0.0015 $\pm$ 1E-4
0.50	0.0011 $\pm$ 1E-4	0.00097 $\pm$ 6E-5	0.0010 $\pm$ 1E-4
0.80	0.00048 $\pm$ 5E-5	0.00049 $\pm$ 5E-5	0.00048 $\pm$ 1E-5
1.30	0.00030 $\pm$ 4E-5	0.00028 $\pm$ 3E-5	0.00029 $\pm$ 1E-5
1.80	0.00018 $\pm$ 2E-5	0.00020 $\pm$ 2E-5	0.00019 $\pm$ 1E-5
2.80	0.00014 $\pm$ 2E-5	0.00013 $\pm$ 1E-5	0.00014 $\pm$ 1E-5
3.80	0.00011 $\pm$ 1E-5	0.00012 $\pm$ 1E-5	0.00011 $\pm$ 1E-5
4.80	0.000086 $\pm$ 8E-6	0.00008 $\pm$ 1E-5	0.000083 $\pm$ 4E-6
6.80	0.000082 $\pm$ 9E-6	0.000086 $\pm$ 8E-6	0.000084 $\pm$ 3E-6
9.00	0.000057 $\pm$ 8E-6	0.000062 $\pm$ 7E-6	0.000059 $\pm$ 3E-6

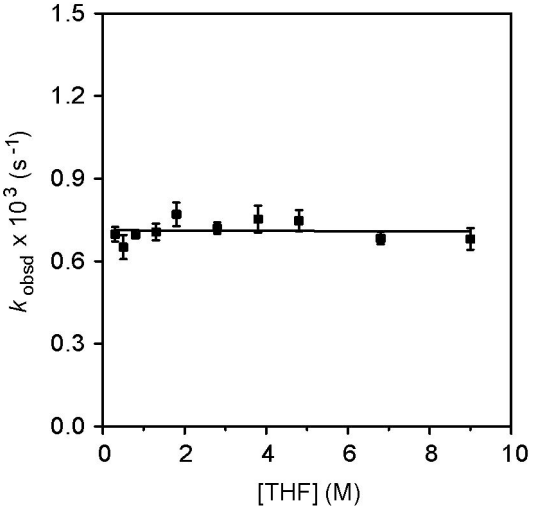

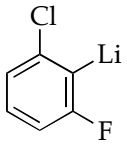

6

XV. Plot of k_{obsd} versus [THF] in toluene cosolvent for the formation of 3-fluorobenzyne (**4b**) from **6** (0.2 M) at -25 °C. The curve depicts the result of an unweighted least-squares fit to $k_{obsd} = k[\text{THF}] + k'$ ($k = -1 \pm 4 \times 10^{-6}$, $k' = 7.1 \pm 0.2 \times 10^{-4}$).

[THF] (M)	$k_{obsd}1$ (s^{-1})	$k_{obsd}2$ (s^{-1})	k_{obsd}av (s^{-1})
0.30	0.00068 ± 6E-5	0.00072 ± 5E-5	0.00070 ± 3E-5
0.50	0.00068 ± 6E-5	0.00062 ± 5E-5	0.00065 ± 4E-5
0.80	0.00069 ± 7E-5	0.00071 ± 7E-5	0.00070 ± 1E-5
1.30	0.00073 ± 8E-5	0.00068 ± 7E-5	0.00070 ± 3E-5
1.80	0.00074 ± 8E-5	0.00080 ± 8E-5	0.00077 ± 4E-5
2.80	0.00073 ± 8E-5	0.00071 ± 6E-5	0.00072 ± 2E-5
3.80	0.00072 ± 7E-5	0.00079 ± 7E-5	0.00075 ± 5E-5
4.80	0.00077 ± 8E-5	0.00072 ± 7E-5	0.00075 ± 4E-5
6.80	0.00067 ± 7E-5	0.00070 ± 5E-5	0.00068 ± 2E-5
9.00	0.00065 ± 8E-5	0.00071 ± 8E-5	0.00068 ± 4E-5

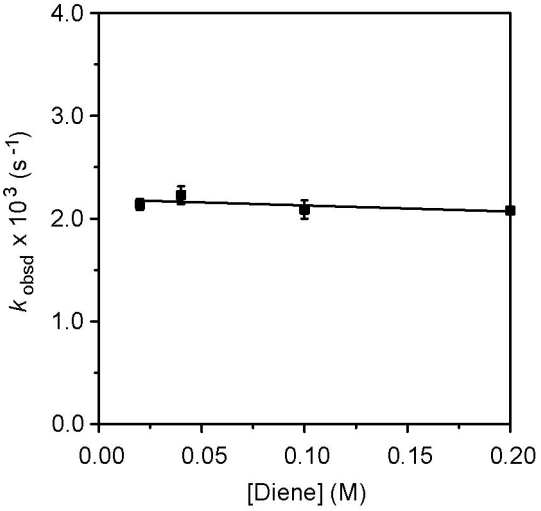

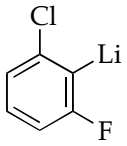

6

XVI. Plot of k_{obsd} versus [spiro[2.4]hepta-4,6-diene] in THF (0.3 M) and toluene cosolvent for the formation of 3-chloro and 3-fluorobenzyne from **6** (0.2 M) at -25 °C. The curve depicts the result of an unweighted least-squares fit to $k_{obsd} = k$[diene] + k' (k = -1 ± 4 x 10^{-4}, k' = 2.2 ± 0.1 x 10^{-3}).

[Diene] (M)	$k_{obsd}1$ (s^{-1})	$k_{obsd}2$ (s^{-1})	k_{obsd}av (s^{-1})
0.02	0.0022 ± 2E-4	0.00212 ± 4E-5	0.00216 ± 5E-5
0.04	0.0022 ± 2E-4	0.0023 ± 2E-4	0.0022 ± 1E-4
0.10	0.0020 ± 1E-4	0.00217 ± 4E-5	0.00211 ± 9E-5
0.20	0.00207 ± 3E-5	0.0021 ± 2E-4	0.00210 ± 4E-5

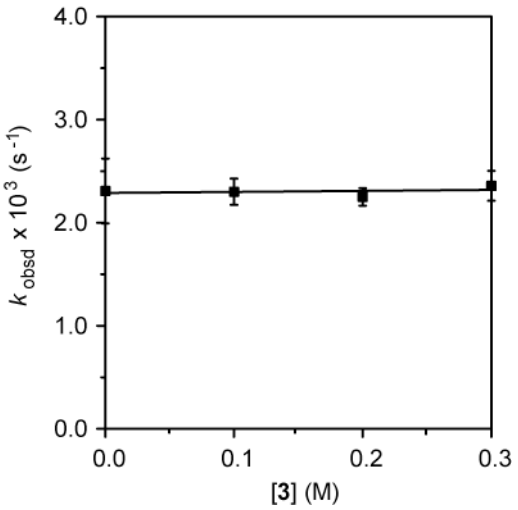

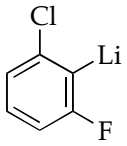

6

XVII. Plot of k_{obsd} versus [**3**] in THF (0.3 M) and toluene cosolvent for the formation of 3-chloro and 3-fluorobenzyne from **6** (0.2 M) at -25 °C. The curve depicts the result of an unweighted least-squares fit to $k_{obsd} = k[\mathbf{3}] + k'$ ($k = 1 \pm 2$ x 10^{-4}, $k' = 2.3 \pm 0.1$ x 10^{-3}).

[**3**] (M)	$k_{obsd}1$ (s^{-1})	$k_{obsd}2$ (s^{-1})	k_{obsd}av (s^{-1})
0.00	0.0025 ± 3E-4	0.0021 ± 2E-4	0.0023 ± 3E-4
0.10	0.0022 ± 2E-4	0.0024 ± 3E-4	0.0023 ± 1E-4
0.20	0.0022 ± 2E-4	0.0023 ± 2E-4	0.0022 ± 1E-4
0.30	0.00225 ± 3E-5	0.0025 ± 2E-4	0.0024 ± 1E-4

XVIII. Table of data for observed ratio of [**5a**]:[**5b**] versus [THF] in toluene cosolvent for the formation of 3-chloro and 3-fluorobenzyne from **6** (0.2 M).

[THF] (M)	[**5a**]:[**5b**] (av)	[THF] (M)	[**5a**]:[**5b**] (av)
0.30	0.69 ± 0.08	2.80	0.16 ± 0.02
0.50	0.61 ± 0.07	3.80	0.13 ± 0.01
0.80	0.41 ± 0.05	4.80	0.10 ± 0.01
1.30	0.29 ± 0.02	6.80	0.11 ± 0.01
1.80	0.20 ± 0.02	9.00	0.08 ± 0.01

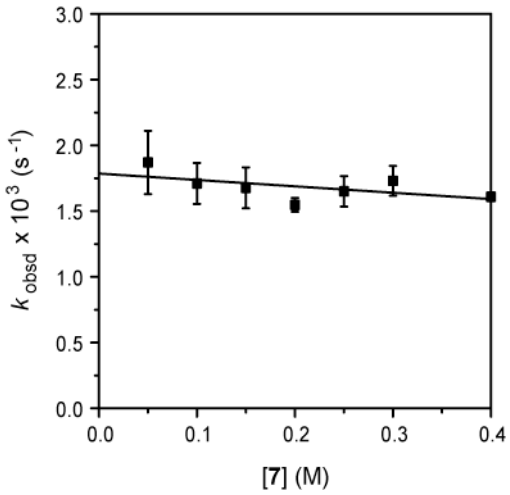

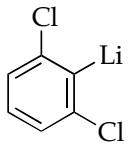

7

XIX. Plot of k_{obsd} versus [**7**] in THF (0.3 M) and toluene cosolvent for the formation of 3-chlorobenzyne (**4a**) at -25 °C. The curve depicts the result of an unweighted least-squares fit to $k_{obsd} = k[\mathbf{7}] + k'$ (k = (-5 ± 3) x 10^{-4}, k' = (1.8 ± 0.1) x 10^{-3}).

[**7**] (M)	$k_{obsd}1$ (s^{-1})	$k_{obsd}2$ (s^{-1})	k_{obsd}av (s^{-1})
0.05	0.0017 ± 1E-4	0.0020 ± 2E-4	0.0019 ± 2E-4
0.10	0.0016 ± 1E-4	0.0018 ± 2E-4	0.0017 ± 1E-4
0.15	0.00179 ± 9E-5	0.0016 ± 1E-4	0.0017 ± 1E-4
0.20	0.0016 ± 2E-4	0.00151 ± 5E-5	0.00155 ± 5E-5
0.25	0.0017 ± 1E-4	0.00157 ± 9E-5	0.0016 ± 1E-4
0.30	0.0016 ± 1E-4	0.00181 ± 8E-5	0.0017 ± 1E-4
0.40	0.00163 ± 7E-5	0.0016 ± 1E-4	0.00161 ± 3E-5

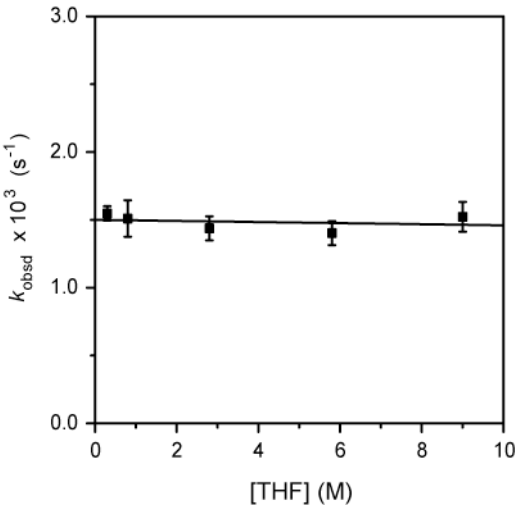

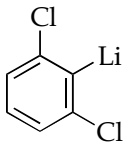

7

XX. Plot of k_{obsd} vs [THF] in toluene cosolvent for the formation of 3-chlorobenzyne (**4a**) from **7** (0.2 M) at -25 °C. The curve depicts the result of an unweighted least-squares fit to $k_{obsd} = k[THF] + k'$ ($k = (-4 \pm 9) \times 10^{-6}$, $k' = (1.5 \pm 0.1) \times 10^{-3}$).

[THF] (M)	$k_{obsd}1$ (s^{-1})	$k_{obsd}2$ (s^{-1})	k_{obsd}av (s^{-1})
0.30	0.0016 ± 2E-4	0.00151 ± 5E-5	0.00155 ± 6E-5
0.80	0.00141 ± 8E-5	0.0016 ± 1E-4	0.0015 ± 1E-4
2.80	0.00137 ± 7E-5	0.0015 ± 1E-4	0.00144 ± 9E-5
5.80	0.0013 ± 1E-4	0.00146 ± 9E-5	0.00140 ± 9E-5
9.00	0.00144 ± 9E-5	0.0016 ± 2E-4	0.0015± 1E-4

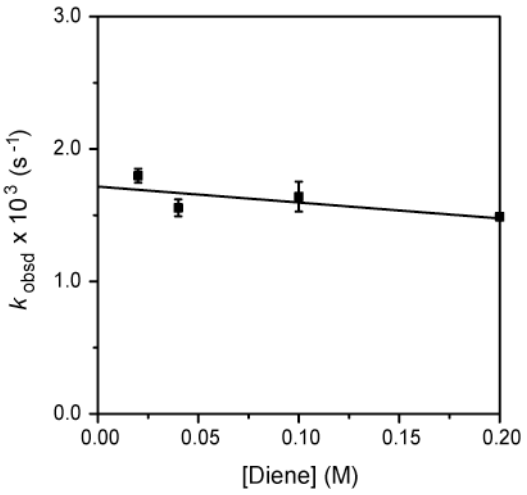

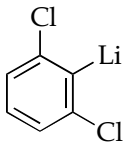

7

XXI. Plot of k_{obsd} versus [spiro[2.4]hepta-4,6-diene] in THF (0.3 M) and toluene cosolvent for the formation of 3-chlorobenzyne (**4a**) from **7** (0.2 M) at -25 °C. The curve depicts the result of an unweighted least-squares fit to $k_{obsd} = k$[diene] + k' (k = (-6 ± 3) x 10^{-4}, k' = (9.4 ± 0.3) x 10^{-4}).

[Diene] (M)	$k_{obsd}1$ (s^{-1})	$k_{obsd}2$ (s^{-1})	k_{obsd}av (s^{-1})
0.02	0.0018 ± 2E-4	0.00183 ± 8E-5	0.00180 ± 5E-5
0.04	0.0016 ± 2E-4	0.00151 ± 5E-5	0.00155 ± 6E-5
0.10	0.00156 ± 8E-5	0.0017 ± 2E-4	0.0016 ± 1E-4
0.20	0.0015 ± 1E-4	0.00147 ± 6E-5	0.00149 ± 2E-5

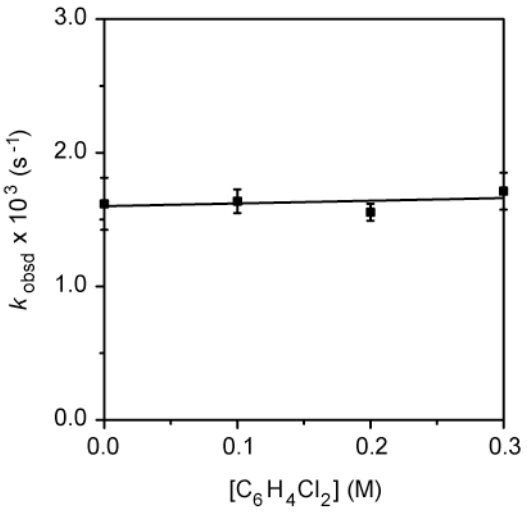

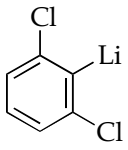

7

XXII. Plot of k_{obsd} versus [$C_6H_4Cl_2$] in THF (0.3 M) and toluene cosolvent for the formation of 3-chlorobenzyne (**4a**) from **7** (0.2 M) at -25 °C. The curve depicts the result of an unweighted least-squares fit to $k_{obsd} = k[C_6H_4Cl_2] + k'$ ($k = 2 \pm 3 \times 10^{-4}$, $k' = 1.6 \pm 0.1 \times 10^{-3}$).

[$C_6H_4Cl_2$] (M)	$k_{obsd}1$ (s^{-1})	$k_{obsd}2$ (s^{-1})	k_{obsd}av (s^{-1})
0.00	0.0017 ± 2E-4	0.00148 ± 8E-5	0.0016 ± 2E-4
0.10	0.00170 ± 7E-5	0.00157 ± 7E-5	0.00164 ± 9E-5
0.20	0.0016 ± 2E-4	0.00151 ± 5E-5	0.00155 ± 6E-5
0.30	0.00161 ± 8E-5	0.0018 ± 1E-4	0.0017 ± 1E-4

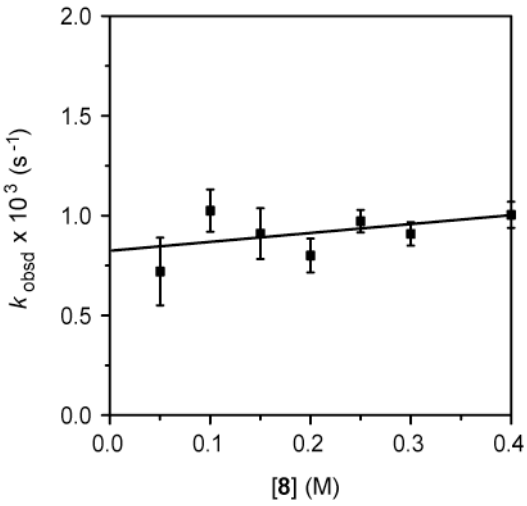

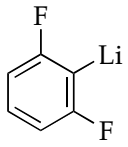

8

XXIII. Plot of k_{obsd} versus [**8**] in THF (0.3 M) and toluene cosolvent for the formation of 3-fluorobenzyne (**4b**) at -25 °C. The curve depicts the result of an unweighted least-squares fit to $k_{obsd} = k[\mathbf{8}] + k'$ ($k = 4.5 \pm 3.6$) x 10^{-4}, $k' = (8 \pm 1)$ x 10^{-4}).

[**8**] (M)	$k_{obsd}1$ (s^{-1})	$k_{obsd}2$ (s^{-1})	k_{obsd}av (s^{-1})
0.05	0.00060 ± 9E-5	0.0008 ± 1E-4	0.0007 ± 2E-4
0.10	0.00095 ± 8E-5	0.0011 ± 1E-4	0.0010 ± 1E-4
0.15	0.00082 ± 9E-5	0.0010 ± 1E-4	0.0009 ± 1E-4
0.20	0.00086 ± 9E-5	0.00074 ± 9E-5	0.00080 ± 8E-5
0.25	0.0010 ± 1E-4	0.00093 ± 7E-5	0.00097 ± 6E-5
0.30	0.00087 ± 8E-5	0.00095 ± 7E-5	0.00091 ± 6E-5
0.40	0.00096 ± 9E-5	0.0010 ± 1E-4	0.0010 ± 1E-4

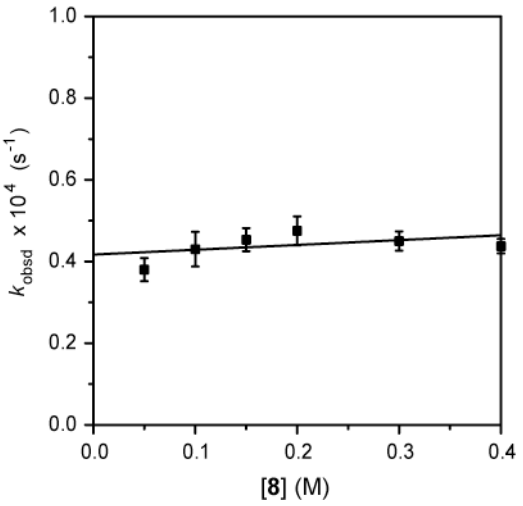

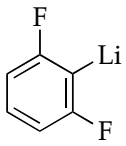

8

XXIV. Plot of k_{obsd} versus [**8**] in THF (6.8 M) and toluene cosolvent for the formation of 3-fluorobenzyne (**4b**) at -25 °C. The curve depicts the result of an unweighted least-squares fit to $k_{obsd} = k[\mathbf{8}] + k'$ ($k = 1 \pm 1$) x 10^{-5}, $k' = (4.1 \pm 0.2)$ x 10^{-5}).

[**8**] (M)	$k_{obsd}1$ (s^{-1})	$k_{obsd}2$ (s^{-1})	k_{obsd}av (s^{-1})
0.05	0.000036 ± 5E-6	0.000040 ± 5E-6	0.000038 ± 3E-6
0.10	0.000040 ± 6E-6	0.000046 ± 6E-6	0.000043 ± 4E-6
0.15	0.000043 ± 3E-6	0.000047 ± 2E-6	0.000045 ± 3E-6
0.20	0.000050 ± 6E-6	0.000045 ± 6E-6	0.000047 ± 3E-6
0.30	0.000047 ± 5E-6	0.000043 ± 6E-6	0.000045 ± 2E-6
0.40	0.000042 ± 4E-6	0.000045 ± 5E-6	0.000044 ± 2E-6

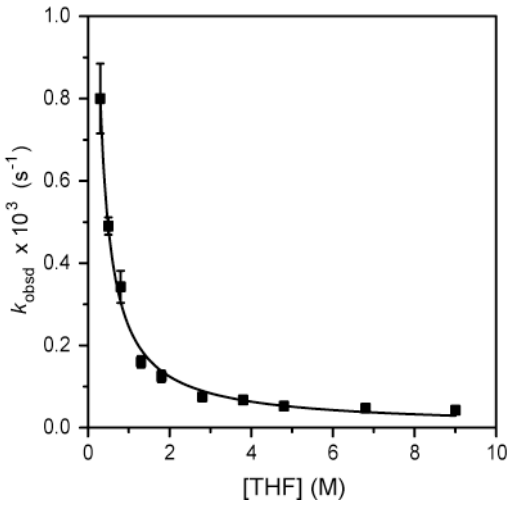

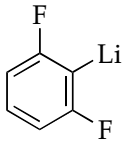

8

XXV. Plot of k_{obsd} versus [THF] in toluene cosolvent for the formation of 3-fluorobenzyne (**4b**) from **8** (0.2 M) at -25 °C. The curve depicts the result of an unweighted least-squares fit to $k_{obsd} = k[THF]^n + k'$ ($k = 2.4 \pm 0.2$) x 10^{-4}, n = -1.0 $\pm$ 0.1, $k' = (0.1 \pm 2.0)$ x 10^{-5}).

[THF] (M)	$k_{obsd}1$ (s^{-1})	$k_{obsd}2$ (s^{-1})	k_{obsd}av (s^{-1})
0.30	0.00086 $\pm$ 9E-5	0.00074 $\pm$ 9E-5	0.00080 $\pm$ 7E-5
0.50	0.00047 $\pm$ 6E-5	0.0005 $\pm$ 1E-4	0.00049 $\pm$ 2E-5
0.80	0.00031 $\pm$ 4E-5	0.00037 $\pm$ 3E-5	0.00034 $\pm$ 4E-5
1.30	0.00017 $\pm$ 2E-5	0.00015 $\pm$ 1E-5	0.00016 $\pm$ 1E-5
1.80	0.00011 $\pm$ 1E-5	0.00013 $\pm$ 1E-5	0.00012 $\pm$ 1E-5
2.80	0.00008 $\pm$ 1E-5	0.00007 $\pm$ 1E-5	0.000075 $\pm$ 4E-6
3.80	0.00007 $\pm$ 1E-5	0.000065 $\pm$ 5E-6	0.000067 $\pm$ 3E-6
4.80	0.000055 $\pm$ 6E-6	0.000050 $\pm$ 7E-6	0.000052 $\pm$ 3E-6
6.80	0.000050 $\pm$ 6E-6	0.000045 $\pm$ 6E-6	0.000047 $\pm$ 3E-6
9.00	0.000041 $\pm$ 4E-6	0.000044 $\pm$ 6E-6	0.000042 $\pm$ 3E-6

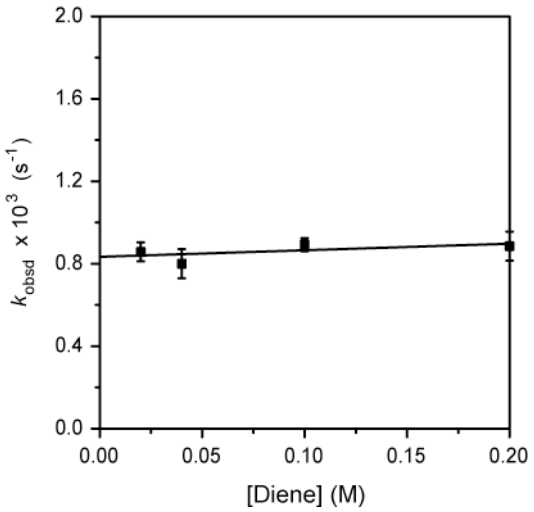

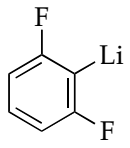

8

XXVI. Plot of k_{obsd} versus [spiro[2.4]hepta-4,6-diene] in THF (0.3 M) and toluene cosolvent for the formation of 3-fluorobenzyne (**4b**) from **8** (0.2 M) at -25 °C. The curve depicts the result of an unweighted least-squares fit to $k_{obsd} = k$[diene] + k' ($k = (3 \pm 3) \times 10^{-4}$, $k' = (8.3 \pm 0.3) \times 10^{-4}$).

[Diene] (M)	$k_{obsd}1$ (s^{-1})	$k_{obsd}2$ (s^{-1})	k_{obsd}av (s^{-1})
0.02	0.00082 ± 8E-5	0.0009 ± 1E-4	0.00086 ± 4E-5
0.04	0.00086 ± 9E-5	0.00074 ± 9E-5	0.00080 ± 7E-5
0.10	0.0009 ± 1E-4	0.00087 ± 9E-5	0.00089 ± 3E-5
0.20	0.0009 ± 1E-4	0.00083 ± 7E-5	0.00088 ± 7E-5

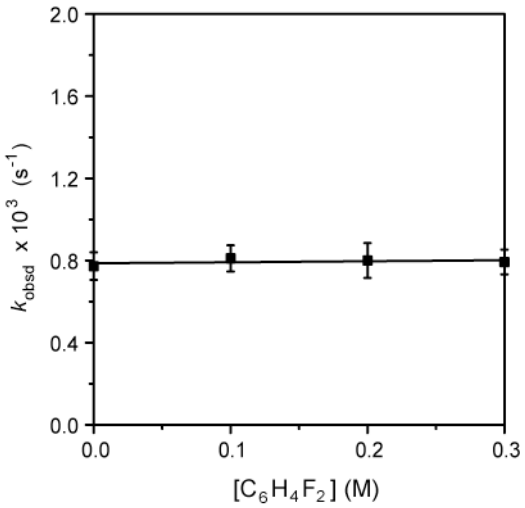

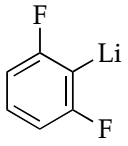

8

XXVII. Plot of k_{obsd} versus [$C_6H_4F_2$] in THF (0.3 M) and toluene cosolvent for the formation of 3-fluorobenzyne (**4b**) from **8** (0.2 M) at -25 ˚C. The curve depicts the result of an unweighted least-squares fit to $k_{obsd} = k[C_6H_4Cl_2] + k'$ ($k = (5 \pm 8) \times 10^{-5}$, $k' = (7.8 \pm 0.1) \times 10^{-4}$).

[$C_6H_4F_2$] (M)	$k_{obsd}1$ (s^{-1})	$k_{obsd}2$ (s^{-1})	k_{obsd}av (s^{-1})
0.00	0.00072 ± 9E-5	0.0008 ± 1E-4	0.00077 ± 7E-5
0.10	0.0008 ± 1E-4	0.00085 ± 8E-5	0.00081 ± 6E-5
0.20	0.00086 ± 9E-5	0.00074 ± 9E-5	0.00080 ± 7E-5
0.30	0.00083 ± 8E-5	0.0007 ± 1E-4	0.00079 ± 6E-5

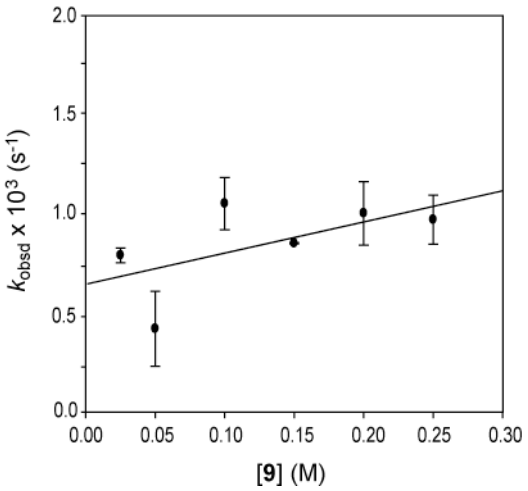

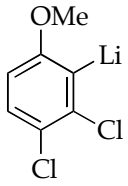

9

XXVIII. Plot of k_{obsd} versus [**9**] in THF (5.0 M) and toluene cosolvent for the formation of 6-chloro-3-methoxybenzyne from **9** at -50 °C. The curve depicts the result of an unweighted least-squares fit to $k_{obsd} = k[\mathbf{9}] + k'$ ($k = (2 \pm 1)$ x 10^{-3}, $k' = (6 \pm 2)$ x 10^{-4}).

[**9**] (M)	$k_{obsd}1$ (s^{-1})	$k_{obsd}2$ (s^{-1})	k_{obsd}av (s^{-1})
0.025	0.00082 ± 9E-5	0.0008 ± 2E-4	0.00079 ± 4E-5
0.050	0.00055 ± 7E-5	0.00029 ± 6E-5	0.0004 ± 2E-4
0.100	0.0011 ± 1E-4	0.0010 ± 1E-4	0.0010 ± 1E-4
0.150	0.0008 ± 1E-4	0.00085 ± 1E-5	0.000850 ± 3E-6
0.200	0.00112 ± 7E-5	0.0009 ± 2E-4	0.0010 ± 2E-4
0.250	0.00082 ± 9E-5	0.0010 ± 1E-4	0.00079 ± 4E-5

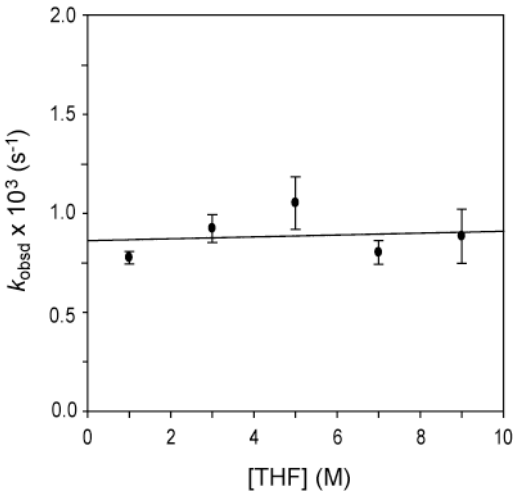

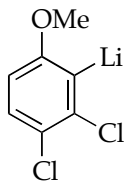

9

XXIX. Plot of k_{obsd} versus [THF] in toluene cosolvent for the formation of 3-chloro-6-methoxybenzyne from **9** (0.1 M) at -50 °C. The curve depicts the result of an unweighted least-squares fit to $k_{obsd} = k[\text{THF}] + k'$ ($k = (0.5 \pm 2.0) \times 10^{-5}$, $k' = (9 \pm 1) \times 10^{-4}$).

[THF] (M)	$k_{obsd}1$ (s^{-1})	$k_{obsd}2$ (s^{-1})	k_{obsd}av (s^{-1})
1.0	0.0007 ± 1E-4	0.00080 ± 5E-5	0.00078 ± 3E-5
3.0	0.00097 ± 6E-5	0.0009 ± 1E-4	0.00092 ± 7E-5
5.0	0.0011 ± 1E-4	0.0010 ± 1E-4	0.0010 ± 1E-4
7.0	0.00076 ± 6E-5	0.0008 ± 1E-4	0.00080 ± 6E-5
9.0	0.00079 ± 8E-5	0.0010 ± 1E-4	0.00088 ± 6E-5

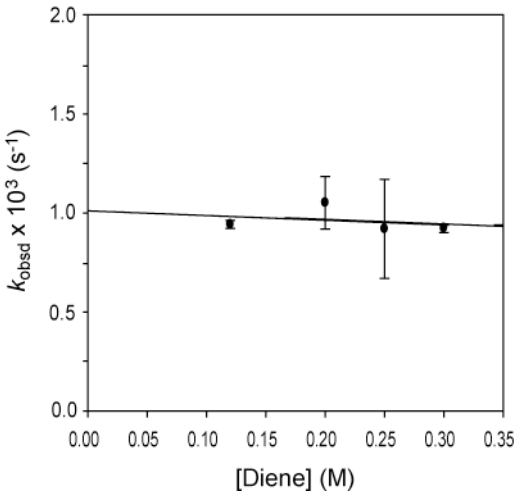

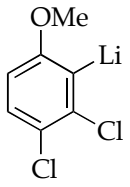

9

XXX. Plot of k_{obsd} versus [spiro[2.4]hepta-4,6-diene] in THF (5.0 M) and toluene cosolvent for the formation of 6-chloro-3-methoxybenzyne from **9** (0.1 M) at -50 °C. The curve depicts the result of an unweighted least-squares fit to $k_{obsd} = k$[diene] + k' (k = (-2 ± 5) x 10^{-4}, k' = (1.0 ± 0.1) x 10^{-3}).

[Diene] (M)	$k_{obsd}1$ (s^{-1})	$k_{obsd}2$ (s^{-1})	k_{obsd}av (s^{-1})
0.12	0.0010 ± 1E-4	0.00093 ± 7E-5	0.00094 ± 2E-5
0.20	0.0011 ± 1E-4	0.0010 ± 1E-4	0.0010 ± 1E-4
0.25	0.0007 ± 1E-4	0.0011 ± 1E-4	0.0009 ± 2E-4
0.30	0.00094 ± 7E-5	0.00091 ± 7E-5	0.00092 ± 2E-5

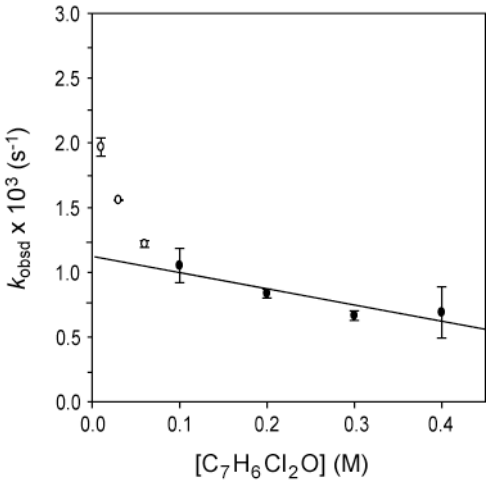

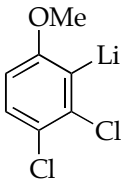

9

XXXI. Plot of k_{obsd} versus [3,4-dichloroanisole] in THF (5.0 M) and toluene cosolvent for the formation of 6-chloro-3-methoxybenzyne from **9** (0.1 M) at -50 °C. The curve depicts the result of an unweighted least-squares fit to $k_{obsd} = k$[3,4-dichloroanisole] + k' (k = (-12 ± 4) x 10^{-4}, k' = (11 ± 1) x 10^{-4}). Points corresponding to [3,4-dichloroanisole] < 0.1 M are represented by and omitted from the fit.

[$C_7H_6Cl_2O$] (M)	$k_{obsd}1$ (s^{-1})	$k_{obsd}2$ (s^{-1})	k_{obsd}av (s^{-1})
0.01	0.0019 ± 1E-4	0.0020 ± 1E-4	0.00197 ± 7E-5
0.03	0.00055 ± 7E-5	0.00156 ± 6E-5	0.0004 ± 2E-4
0.06	0.0012 ± 1E-4	0.0012 ± 1E-4	0.00122 ± 3E-5
0.10	0.0011 ± 1E-4	0.0010 ± 1E-4	0.0010 ± 1E-4
0.20	0.0008 ± 1E-4	0.0009 ± 1E-4	0.00084 ± 4E-5
0.30	0.00069 ± 4E-5	0.00064 ± 3E-5	0.00066 ± 4E-5
0.40	0.0005 ± 2E-4	0.0008 ± 1E-4	0.0007 ± 2E-4

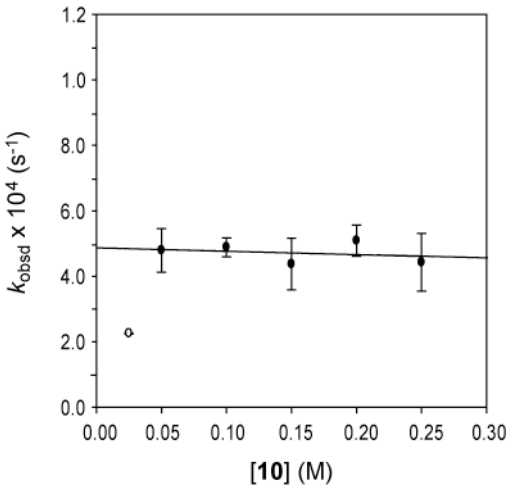

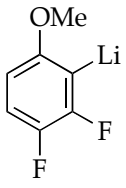

10

XXXII. Plot of k_{obsd} versus [**10**] in THF (5.0 M) and toluene cosolvent for the formation of 6-fluoro-3-methoxybenzyne at -35 °C. The curve depicts the result of an unweighted least-squares fit to $k_{obsd} = k$[**10**] + k' (k = (-1 ± 2) x 10^{-4}, k' = (5 ± 3) x 10^{-4}). A point corresponding to [**10**] = 0.025 M is represented by and omitted from the fit.

[**10**] (M)	$k_{obsd}1$ (s^{-1})	$k_{obsd}2$ (s^{-1})	k_{obsd}av (s^{-1})
0.025	0.00022 ± 5E-5	0.00023 ± 4E-5	0.00023 ± 1E-5
0.050	0.00053 ± 5E-5	0.00043 ± 5E-5	0.00048 ± 7E-5
0.100	0.00051 ± 6E-5	0.00047 ± 4E-5	0.00049 ± 3E-5
0.150	0.00049 ± 1E-5	0.00038 ± 1E-5	0.00044 ± 8E-5
0.200	0.00048 ± 8E-5	0.00054 ± 8E-5	0.00051 ± 4E-5
0.250	0.0005 ± 2E-4	0.00038 ± 8E-5	0.00044 ± 9E-5

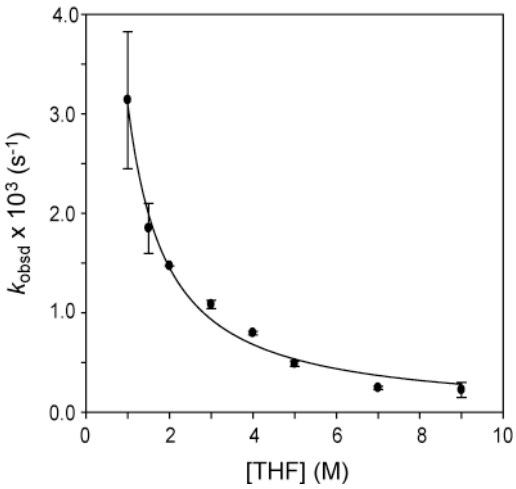

XXXIII. Plot of k_{obsd} versus [THF] in toluene cosolvent for the formation of 6-fluoro-3-methoxybenzyne from **10** (0.1M) at -35 °C. The curve depicts the result of an unweighted least-squares fit to $k_{obsd} = k[THF]^n$ ($k = (3.1 \pm 0.3) \times 10^{-3}$, $n = -1.1 \pm 0.1$).

[THF] (M)	$k_{obsd}1$ (s^{-1})	$k_{obsd}2$ (s^{-1})	k_{obsd}av (s^{-1})
1.0	0.0036 ± 5E-4	0.003 ± 1E-3	0.0031 ± 7E-4
1.5	0.0017 ± 5E-4	0.0020 ± 3E-4	0.00108 ± 4E-5
2.0	0.0014 ± 1E-4	0.00147 ± 8E-5	0.00145 ± 4E-5
3.0	0.00111 ± 6E-5	0.00105 ± 1E-5	0.00108 ± 4E-5
4.0	0.00081 ± 8E-5	0.00078 ± 6E-5	0.00080 ± 2E-5
5.0	0.00051 ± 6E-5	0.00047 ± 4E-5	0.00049 ± 3E-5
7.0	0.00026 ± 5E-5	0.00023 ± 4E-5	0.00024 ± 2E-5
9.0	0.00028 ± 2E-5	0.00012 ± 2E-5	0.00022 ± 1E-5

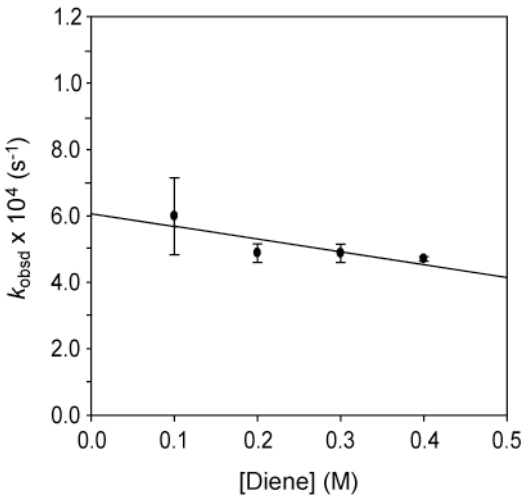

XXXIV. Plot of k_{obsd} versus [spiro[2.4]hepta-4,6-diene] in THF (5.0 M) and toluene cosolvent for the formation of 6-fluoro-3-methoxybenzyne from **10** (0.1 M) at -35 °C. The curve depicts the result of an unweighted least-squares fit to $k_{obsd} = k[\text{diene}] + k'$ ($k = (-4 \pm 2) \times 10^{-4}$, $k' = (6.1 \pm 0.5) \times 10^{-4}$).

[Diene] (M)	$k_{obsd}1$ (s^{-1})	$k_{obsd}2$ (s^{-1})	k_{obsd}av (s^{-1})
0.10	0.00052 ± 6E-5	0.00068 ± 9E-5	0.0006 ± 1E-4
0.20	0.00051 ± 6E-5	0.00047 ± 4E-5	0.00049 ± 3E-5
0.30	0.00051 ± 7E-5	0.00051 ± 4E-5	0.000510 ± 4E-6
0.40	0.0005 ± 1E-4	0.0005 ± 1E-4	0.000470 ± 6E-6

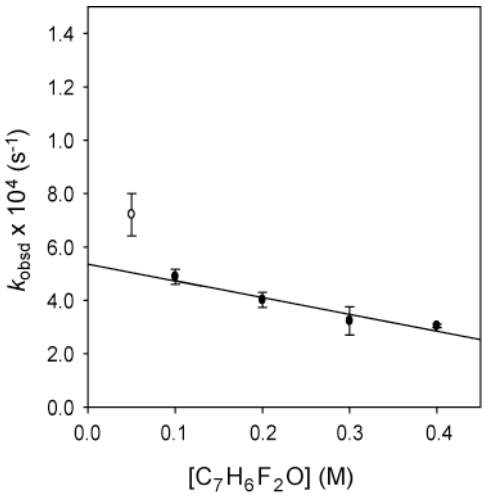

XXXV. Plot of k_{obsd} versus [3,4-difluoroanisole] in THF (5.0 M) and toluene cosolvent for the formation of 3-fluoro-6-methoxybenzyne from **10** (0.1M) at -35 °C. The curve depicts the result of an unweighted least-squares fit to $k_{obsd} = k$[3,4-dichloroanisole] $+ k'$ ($k = (-6 \pm 1) \times 10^{-4}$, $k' = (5.4 \pm 0.3) \times 10^{-4}$). A point corresponding to [3,4-difluoroanisole] = 0.05 M is represented by and omitted from the fit.

[$C_7H_6F_2O$] (M)	$k_{obsd}1$ (s^{-1})	$k_{obsd}2$ (s^{-1})	k_{obsd}av (s^{-1})
0.05	0.00078 ± 5E-5	0.00067 ± 6E-5	0.00072 ± 8E-5
0.10	0.00051 ± 6E-5	0.00047 ± 4E-5	0.00049 ± 3E-5
0.20	0.00042 ± 1E-5	0.00038 ± 5E-5	0.00040 ± 3E-5
0.30	0.00036 ± 5E-5	0.00029 ± 6E-5	0.00032 ± 5E-5
0.40	0.00030 ± 4E-5	0.00031 ± 4E-5	0.000300 ± 6E-6

XXXVI. Optimized geometries[a] and free energies (*G*, Hartrees) of reactants. Free energies (Δ*G*, kcal/mol) include thermal corrections at 298 °C. All calculations were performed with Gaussian 03.[b] Δ*G* Me_2O = -154.97011 Hartrees.

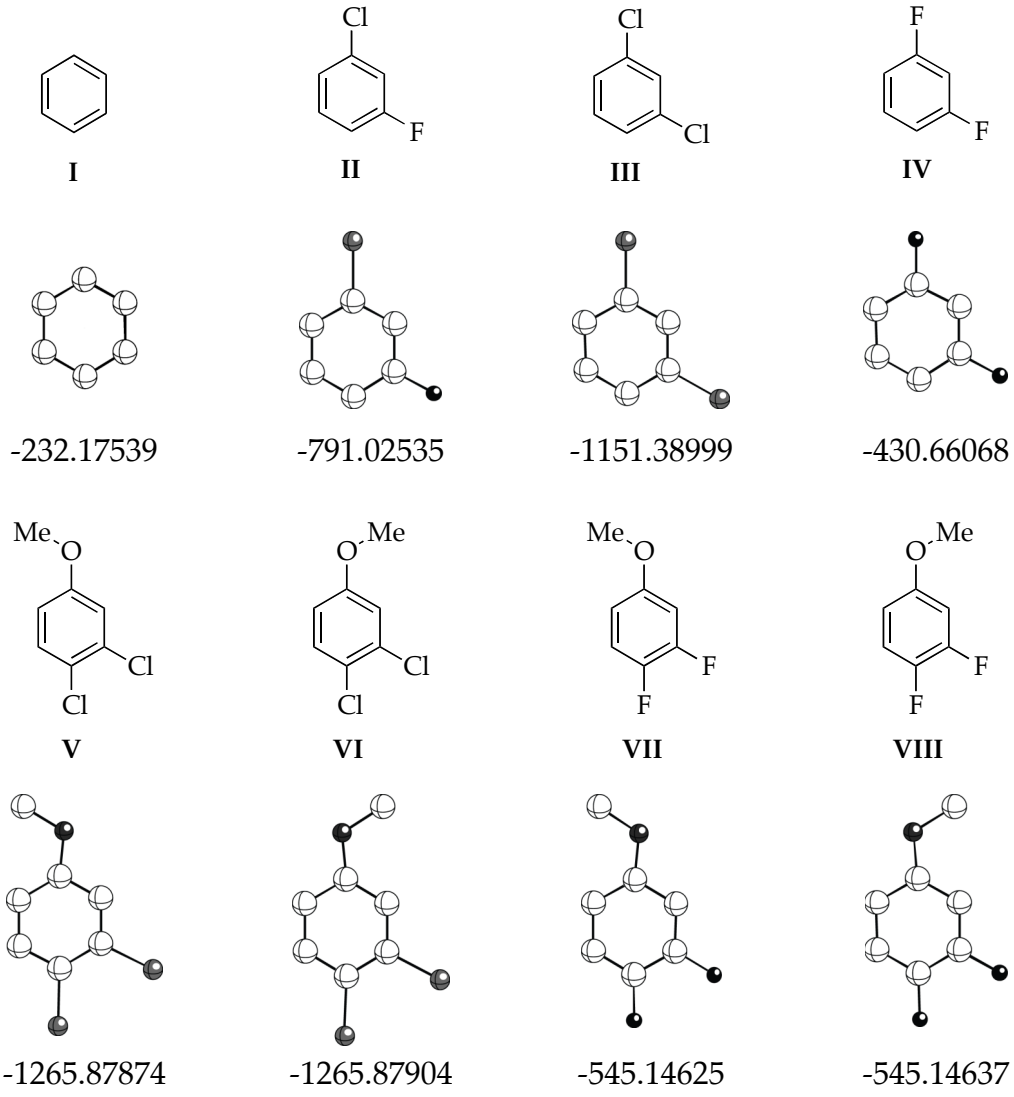

[a]Hydrogens hidden for clarity

[b]Gaussian 03, Revision B.04, Frisch, M. J.; Trucks, G. W.; Schlegel, H. B.; Scuseria, G. E.; Robb, M. A.; Cheeseman, J. R.; Montgomery, Jr., J. A.; Vreven, T.; Kudin, K. N.; Burant, J. C.; Millam, J. M.; Iyengar, S. S.; Tomasi, J.; Barone, V.; Mennucci, B.; Cossi, M.; Scalmani, G.; Rega, N.; Petersson, G. A.; Nakatsuji, H.; Hada, M.; Ehara, M.; Toyota, K.; Fukuda, R.; Hasegawa, J.; Ishida, M.; Nakajima, T.; Honda, Y.; Kitao, O.; Nakai, H.; Klene, M.; Li, X.; Knox, J. E.; Hratchian, H. P.; Cross, J. B.; Bakken, V.; Adamo, C.; Jaramillo, J.; Gomperts, R.; Stratmann, R. E.; Yazyev, O.; Austin, A. J.; Cammi, R.; Pomelli, C.; Ochterski, J. W.; Ayala, P. Y.; Morokuma, K.; Voth, G. A.; Salvador, P.; Dannenberg, J. J.; Zakrzewski, V. G.; Dapprich, S.; Daniels, A. D.; Strain, M. C.; Farkas, O.; Malick, D. K.; Rabuck, A. D.; Raghavachari, K.; Foresman, J. B.; Ortiz, J. V.; Cui, Q.; Baboul, A. G.; Clifford, S.; Cioslowski, J.; Stefanov, B. B.; Liu, G.; Liashenko, A.; Piskorz, P.; Komaromi, I.; Martin, R. L.; Fox, D. J.; Keith, T.; Al-Laham, M. A.; Peng, C. Y.; Nanayakkara, A.; Challacombe, M.; Gill, P. M. W.; Johnson, B.; Chen, W.; Wong, M. W.; Gonzalez, C.; and Pople, J. A.; Gaussian, Inc., Wallingford CT, 2004.

XXXVI (*Continued*).

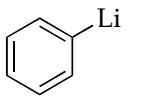

IX

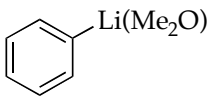

X

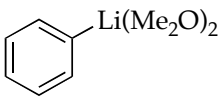

XI

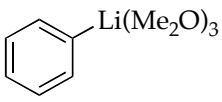

XII

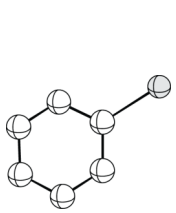

-239.07864

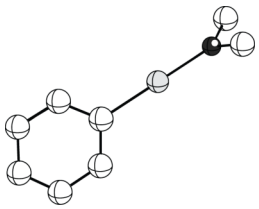

-394.07111

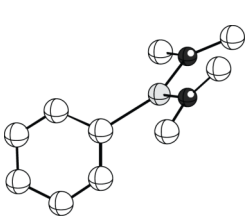

-549.04815

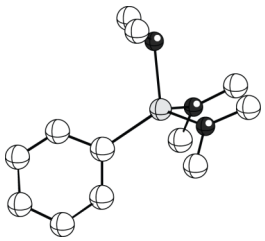

-704.01332

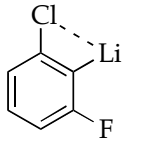

XIII

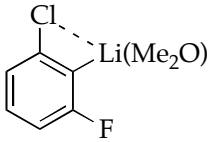

XIV

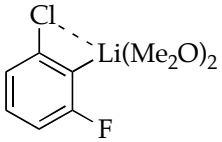

XV

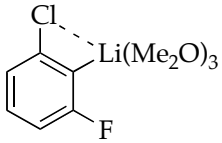

XVI

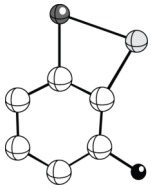

-797.95972

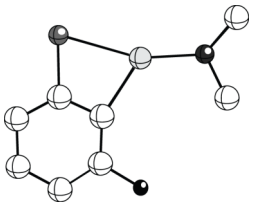

-952.95287

not found[a]

not found[b]

[a]Full optimization of structure **XV** spontaneously converged to its isomer **XIX**.

[b]Full optimization of structure **XVI** spontaneously converged to its isomer **XX**.

XXXVI (*Continued*).

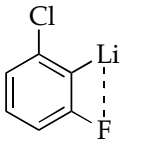

XVII

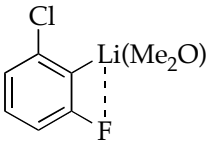

XVIII

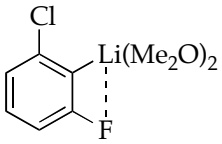

XIX

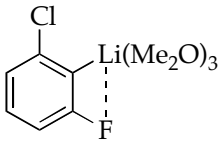

XX

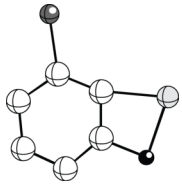

-797.96263

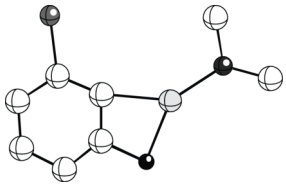

-952.95385

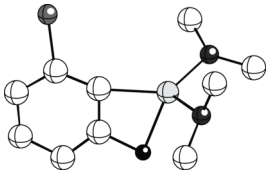

-1107.93083

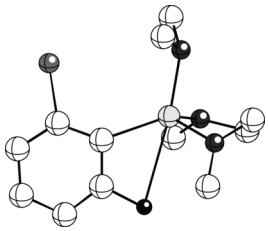

-1262.89376

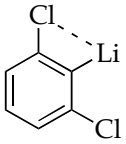

XXI

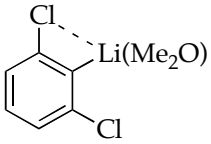

XXII

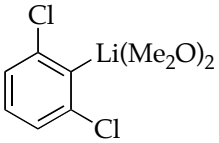

XXIII

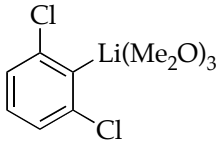

XXIV

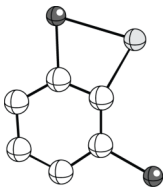

-1158.32343

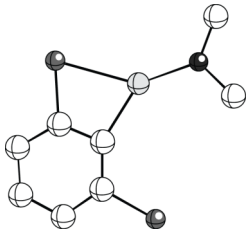

-1313.31444

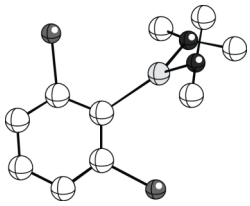

-1468.2924[c]

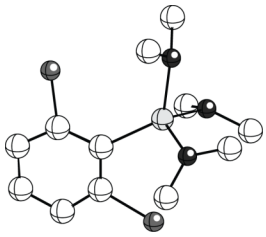

-1623.25413

[c]Most stable conformer shown.

XXXVI (*Continued*).

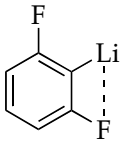

XXV

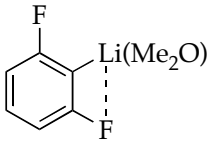

XXVI

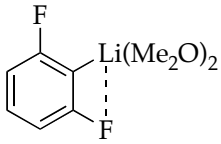

XXVII

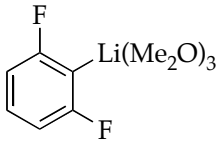

XXVIII

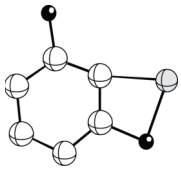

-437.59885

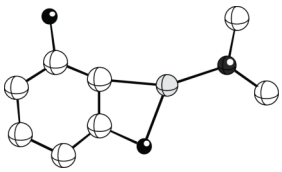

-592.59177

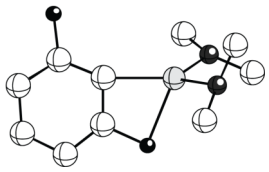

-747.56659

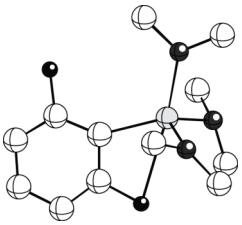

-902.53278[d]

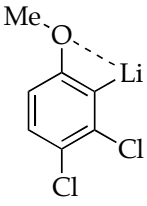

XXIX

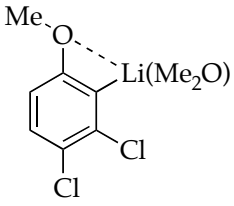

XXX

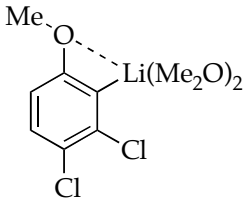

XXXI

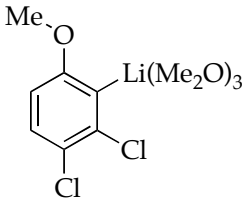

XXXII

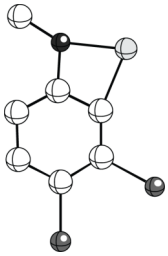

-1272.81491

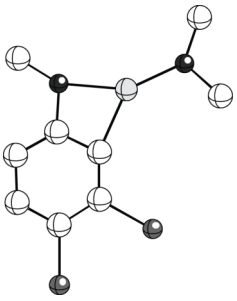

-1427.80448

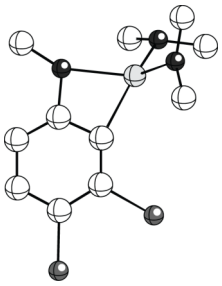

-1582.77960

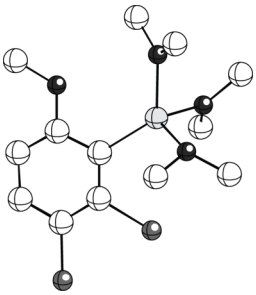

-1737.74130

[d]Isomers without Li-F contacts are minima and display comparable stabilities.

XXXVI (*Continued*).

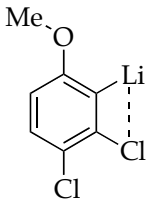

XXXIII

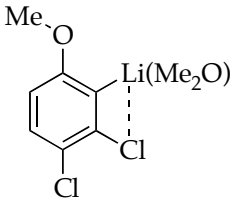

XXXIV

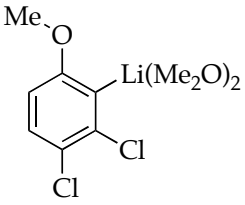

XXXV

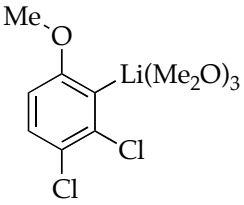

XXXVI

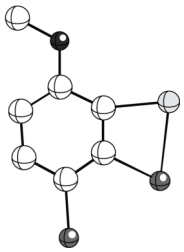

-1272.81107

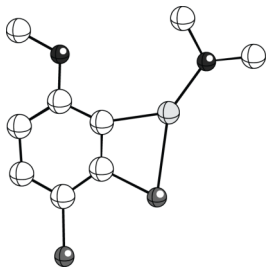

-1427.80159

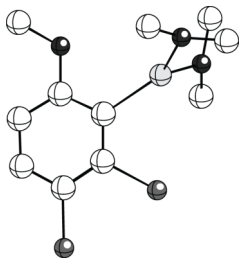

-1582.77785

not found[e]

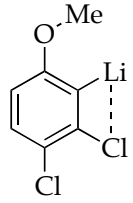

XXXVII

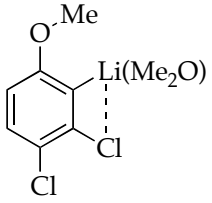

XXXVIII

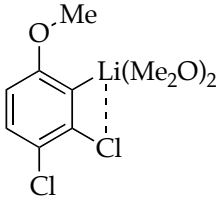

XXXIX

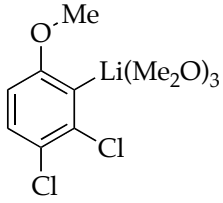

XL

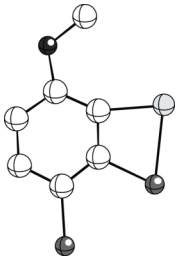

-1272.81270

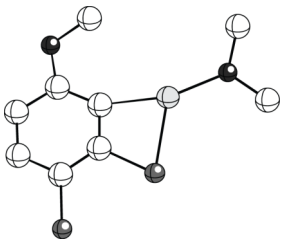

-1427.80316

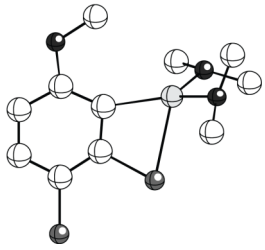

-1582.77770

not found[f]

[e]Full optimization of structure **XL** spontaneously converged to its isomer **XXXII**.

[f]Multiple optimization attempts resulted in dissociation of a Me_2O molecule.

XXXVI (*Continued*).

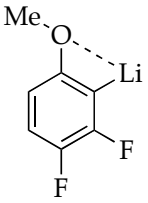

XLI

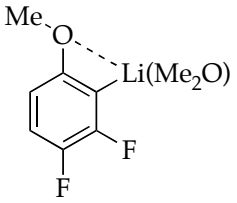

XLII

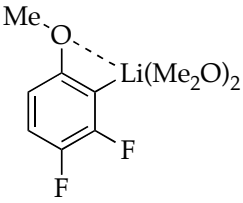

XLIII

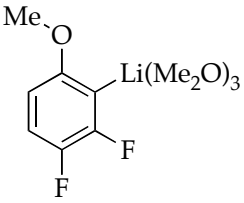

XLIV

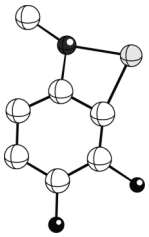

-552.08392

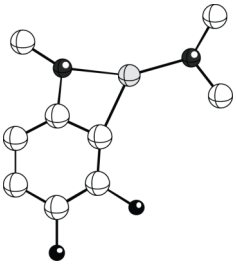

-707.07249

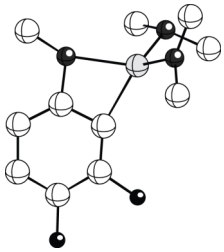

-862.04710

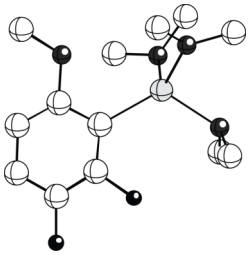

-1017.01273

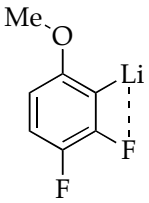

XLV

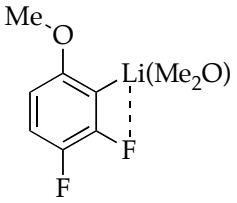

XLVI

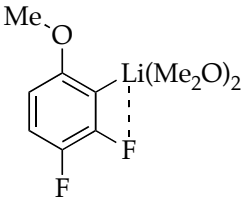

XLVII

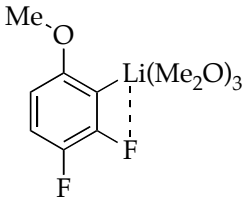

XLVIII

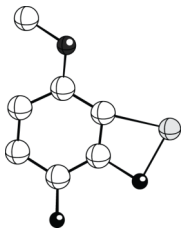

-552.08125

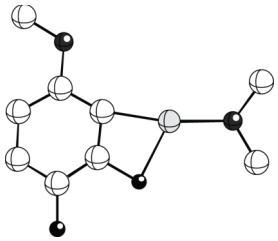

-707.07249

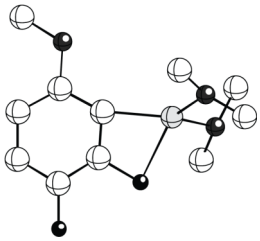

-862.04868

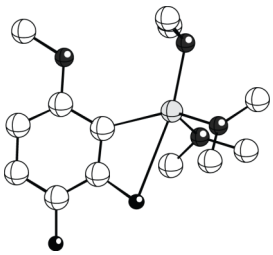

-1017.01277

XXXVI (*Continued*).

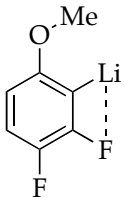

XLIX

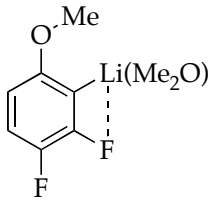

L

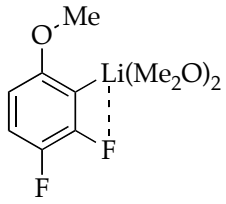

LI

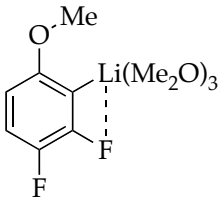

LII

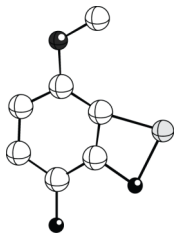

-552.08427

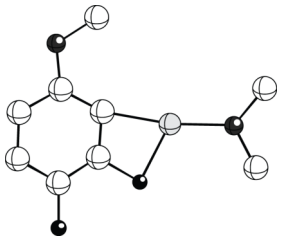

-707.07509

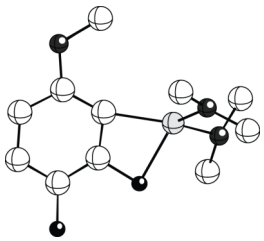

-862.04989

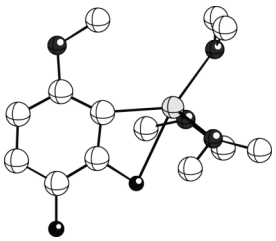

-1017.00975

XXXVII. Selected bond distances (Å) for structures in Section XXXVI.

	C1-C2	C1-C6	C2-C3	C5-C6	C1-X	C2-X	C3-X	C6-X	C5-O	C1-Li	Li-S	Li-X	Li-OMe
I	1.40	---	---	---	---	---	---	---	---	---	---	---	---
II	1.39	---	1.39	---	1.76	---	1.35[a]	---	---	---	---	---	---
III	1.39	---	---	---	1.76	---	---	---	---	---	---	---	---
IV	1.39	---	---	---	---	---	1.35[a]	---	---	---	---	---	---
V	---	1.39	---	1.40	1.75[b]	---	---	---	1.36	---	---	---	---
VI	---	1.40	---	1.40	1.75[b]	---	---	---	1.36	---	---	---	---
VII	---	1.38	---	1.40	1.34[a]	---	---	---	1.36	---	---	---	---
VIII	---	1.39	---	1.40	1.34[a]	---	---	---	1.36	---	---	---	---
IX	1.41	---	---	---	---	---	---	---	---	1.97	---	---	---
X	1.42	---	---	---	---	---	---	---	---	1.99	1.89	---	---
XI	1.42	---	---	---	---	---	---	---	---	2.04	1.95[c]	---	---
XII	1.42	---	---	---	---	---	---	---	---	2.09	2.04[c]	---	---
XIII	1.38	1.39	---	---	---	1.88[b]	---	1.36[a]	---	1.97	---	2.40[d]	---
XIV	1.39	1.39	---	---	---	1.82[b]	---	1.38[b]	---	2.02	1.89	2.49[d]	---
XVII	1.39	1.37	---	---	---	1.79[b]	---	1.46[a]	---	1.98	---	1.90[e]	---
XVIII	1.39	1.37	---	---	---	---	---	1.45[a]	---	2.01	1.88	1.95[e]	---
XIX	1.39	1.38	---	---	---	---	---	1.43[a]	---	2.06	1.95[c]	2.11[e]	---
XX	1.39	1.39	---	---	---	1.80[b]	---	1.40[a]	---	2.12	2.05[c]	2.83[e]	---
XXI	1.38	1.39	---	---	---	1.87[b]	---	1.79[b]	---	1.98	---	2.42[d]	---
XXII	1.38	1.39	---	---	---	1.86[b]	---	1.80[b]	---	2.01	1.88	2.53[d]	---
XXIII	1.39	1.39	---	---	---	1.82[b]	---	1.82[b]	---	2.05	1.95[c]	3.39[d]	---
XXIV	1.39	1.39	---	---	---	1.83[b]	---	1.82[b]	---	2.13	2.04[c]	3.37[d]	---
XXV	1.37	1.39	---	---	---	1.46[a]	---	1.36[a]	---	1.98	---	1.89[e]	---
XXVI	1.37	1.39	---	---	---	1.45[a]	---	1.36[a]	---	2.00	1.89	1.95[e]	---
XXVII	1.37	1.39	---	---	---	1.44[a]	---	1.37[a]	---	2.05	1.95[c]	2.11[e]	---
XXVIII	1.38	1.39	---	---	---	1.40[a]	---	1.39[a]	---	2.10	2.05[c]	2.69[e]	---
XXIX	1.38	1.39	1.41	---	---	1.78[b]	1.76[b]	---	1.43[f]	1.98	---	---	1.93
XXX	1.38	1.40	1.41	---	---	1.79[b]	1.76[b]	---	1.43[f]	2.02	1.89	---	1.99
XXXI	1.38	1.40	1.41	---	---	1.79[b]	1.76[b]	---	1.42[f]	2.06	1.96[c]	---	2.14
XXXII	1.38	1.41	1.41	---	---	1.82[b]	1.77[b]	---	1.39[f]	2.13	2.05[c]	---	3.15
XXXIII	1.37	1.41	1.40	---	---	1.86[b]	1.76[b]	---	1.37[f]	1.97	---	2.41[d]	---
XXXIV	1.37	1.40	1.40	---	---	1.85[b]	1.76[b]	---	1.38[f]	2.00	1.88	2.51[d]	---
XXXV	1.38	1.40	1.40	---	---	1.81[b]	1.76[b]	---	1.40[f]	2.05	1.95[c]	---	---
XXXVII	1.38	1.40	1.39	---	---	1.87[b]	1.76[b]	---	1.37[f]	1.97	---	2.35[d]	---
XXXVIII	1.38	1.40	1.39	---	---	1.86[b]	1.76[b]	---	1.39[f]	2.01	1.90	2.44[d]	---
XXXIX	1.38	1.40	1.40	---	---	1.84[b]	1.76[b]	---	1.38[f]	2.06	1.96[c]	2.61[d]	---
XLI	1.36	1.41	1.39	---	---	1.45[a]	1.35[a]	---	1.38[f]	1.98	---	1.90[e]	1.92
XLII	1.36	1.41	1.39	---	---	1.44[a]	1.35[a]	---	1.38[f]	2.01	1.89	1.97[e]	1.99
XLIII	1.36	1.41	1.39	---	---	1.43[a]	1.36[a]	---	1.39[f]	2.05	1.95[c]	2.13[e]	2.10
XLIV	1.37	1.41	1.40	---	---	1.40[a]	1.36[a]	---	1.40[f]	2.11	2.04[c]	2.88[e]	3.21
XLV	1.36	1.41	1.39	---	**---**	1.45[a]	1.35[a]	---	1.38[f]	1.98	---	1.90[e]	---
XLVI	1.36	1.41	1.39	---	**---**	1.44[a]	1.35[a]	---	1.38[f]	2.01	1.89	1.97[e]	---
XLVII	1.36	1.41	1.39	---	**---**	1.43[a]	1.36[a]	---	1.39[f]	2.05	1.95[c]	2.13[e]	---
XLVIII	1.38	1.41	1.40	---	**---**	1.39[a]	1.36[a]	---	1.40[f]	2.11	2.04[c]	3.25[e]	---
XLIX	1.37	1.40	1.38	---	---	1.45[a]	1.35[a]	---	1.38[f]	1.98	---	1.87[e]	---
L	1.37	1.40	1.38	---	---	1.44[a]	1.35[a]	---	1.38[f]	2.01	1.89	1.94[e]	---
LI	1.37	1.40	1.39	---	---	1.43[a]	1.36[a]	---	1.38[f]	2.07	1.96[c]	2.04[e]	---
LII	1.38	1.40	1.39	---	---	1.41[a]	1.36[a]	---	1.39[f]	2.12	2.08[c]	2.48[e]	---

X=halogen, S = MeO_2.
[a]C-F, [b]C-Cl, [c]Average distance, [d]Li-Cl, [e]Li-F.

XXXVIII. Relaxed PES scans representing potential energy (Δ*E*, kcal/mol) as a function of C-halogen bond lengthening (Å) relative to fully optimized reactants.

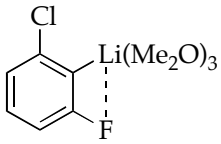

XX

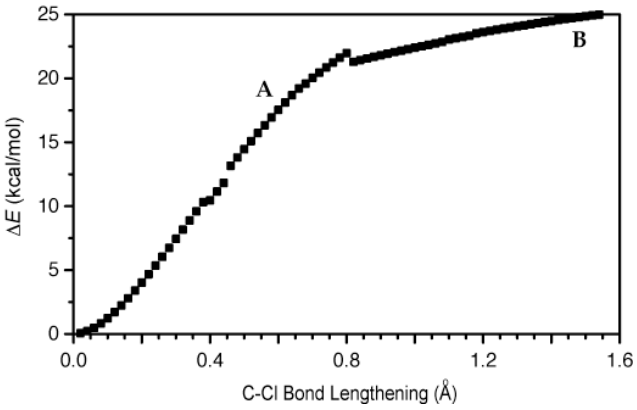

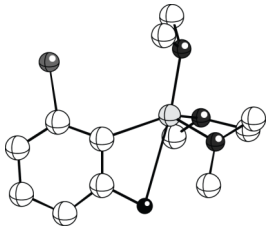

XX

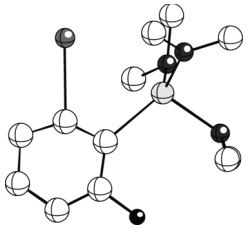

A[a]

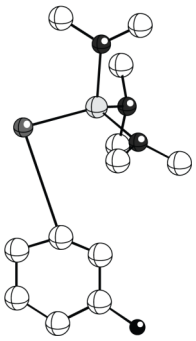

B

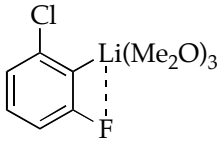

XX

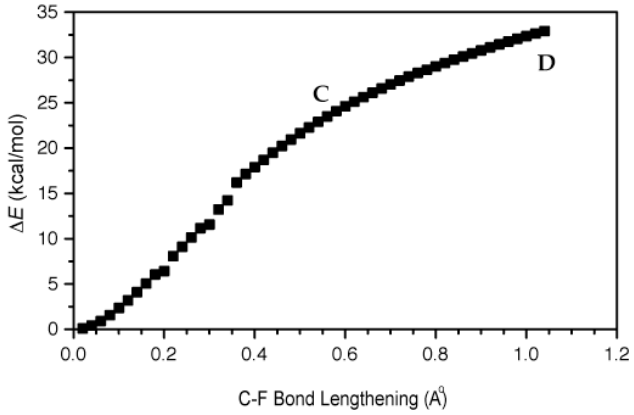

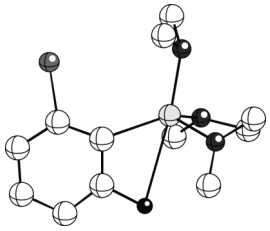

XX

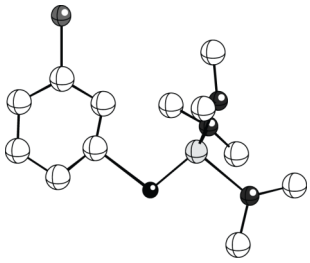

C

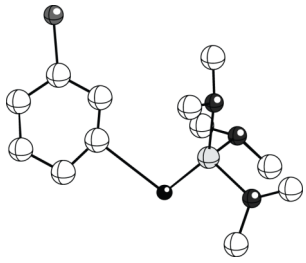

D

[a]Lengthened C-halogen distances shown for clarity.

XXXVIII *(Continued).*

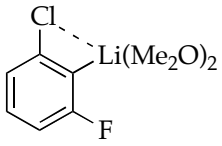

XV

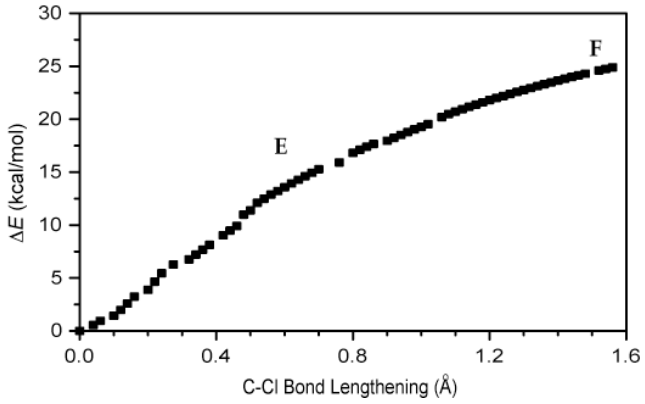

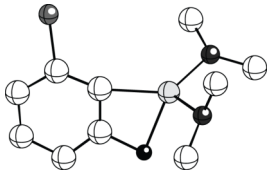

XX[b]

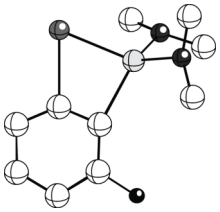

E

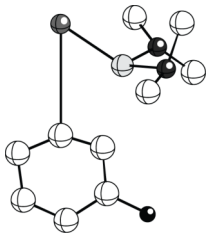

F

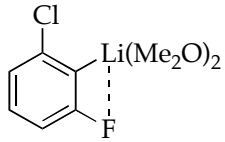

XIX

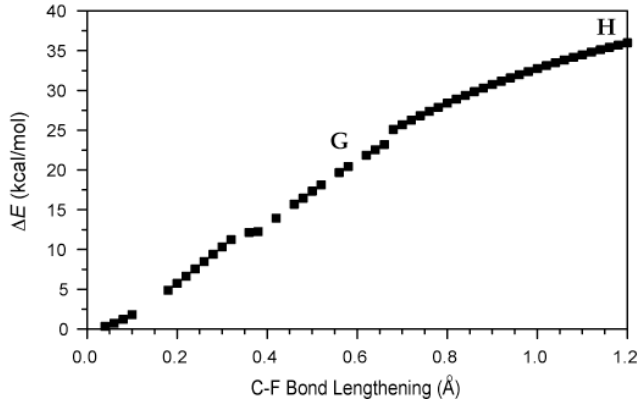

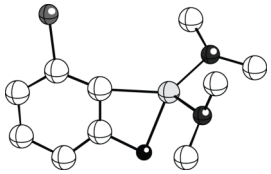

XIX

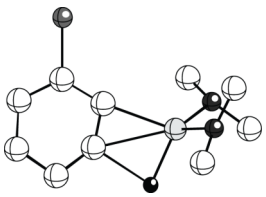

G

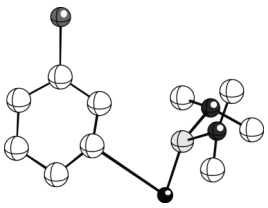

H

[b]Since full optimizations of **XX** with Li-Cl contacts spontaneously converged to its isomer **XX**, Δ*E*'s were normalized to the potential energy and C-Cl bond distance of **XX**.

XXXVIII *(Continued).*

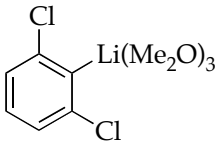

XXIV

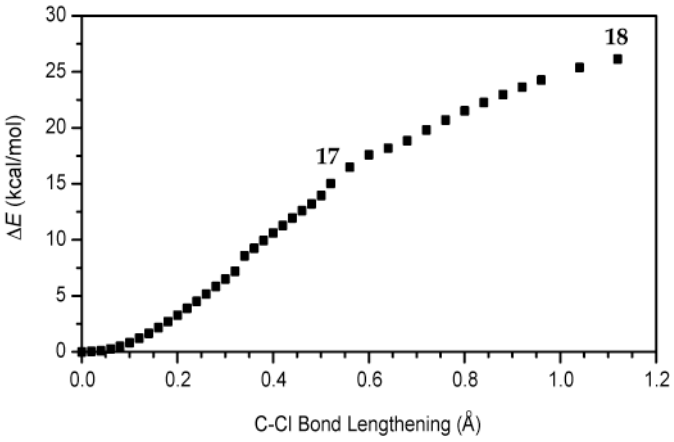

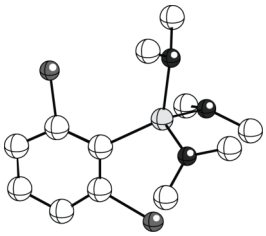

XXIV

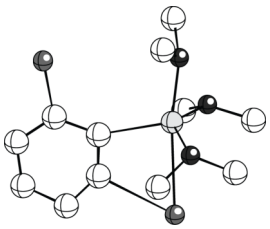

17

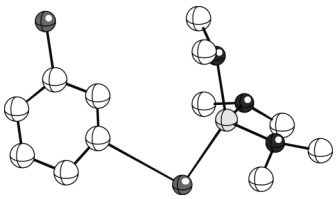

18

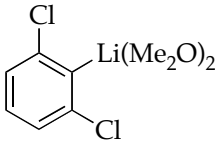

XXIII

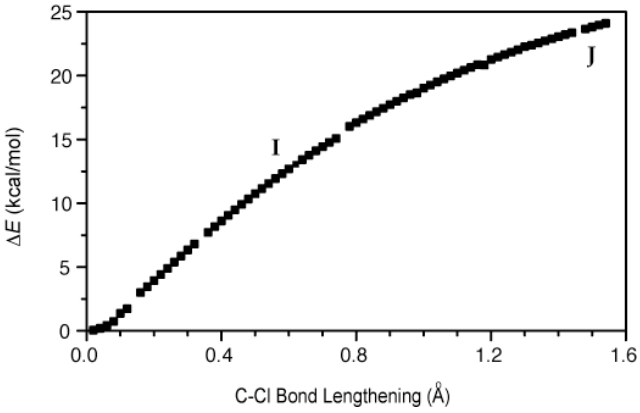

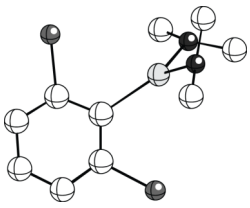

XXIII

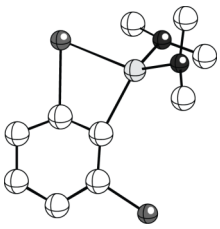

I

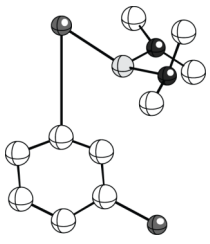

J

XXXVIII *(Continued).*

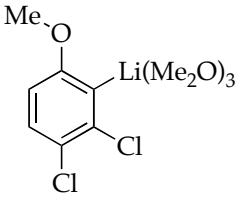

XXXII

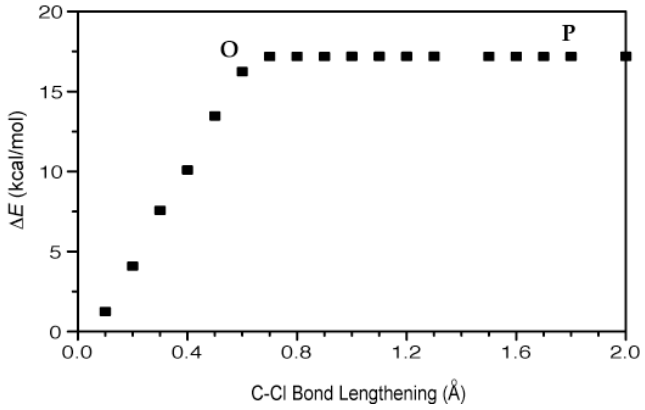

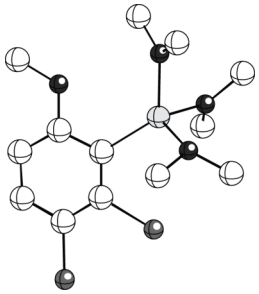

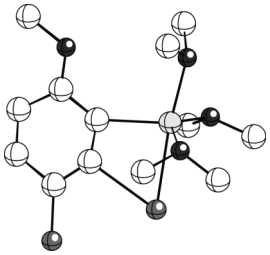

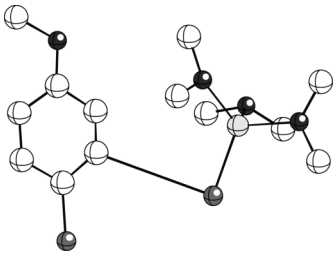

XXXII **O** **P**

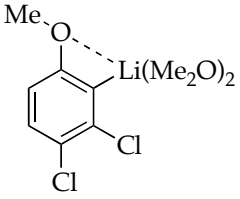

XXXI

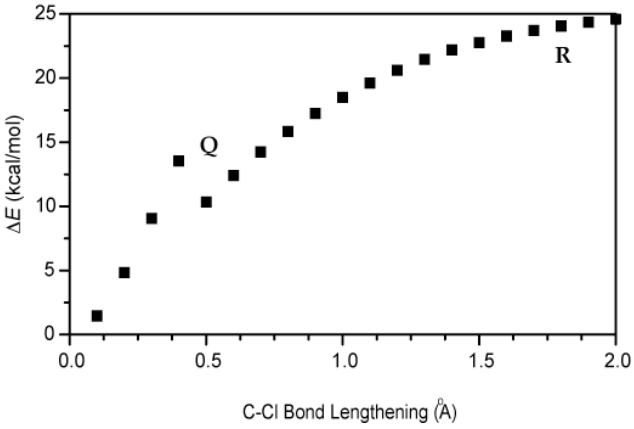

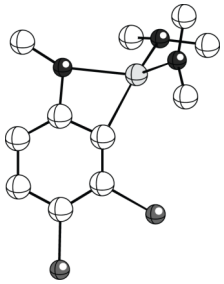

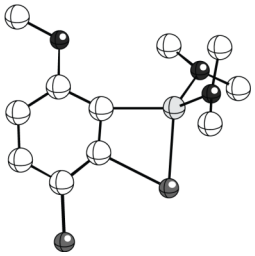

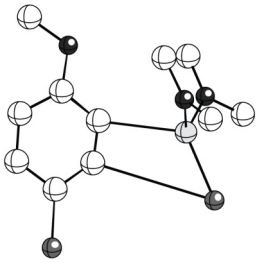

XXXI **Q** **R**

XXXVIII *(Continued).*

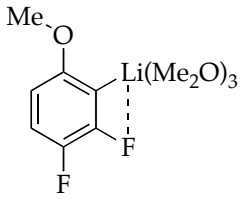

XLVIII

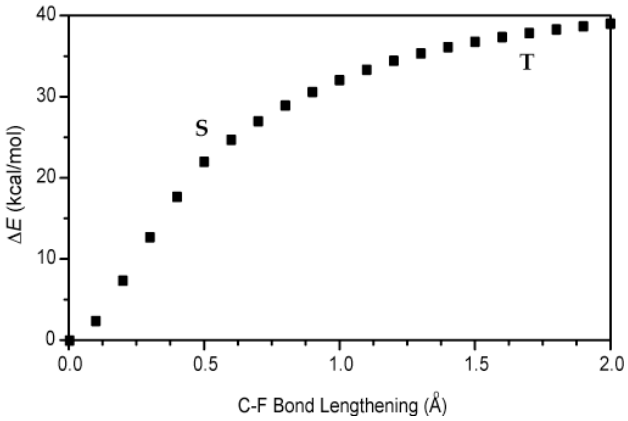

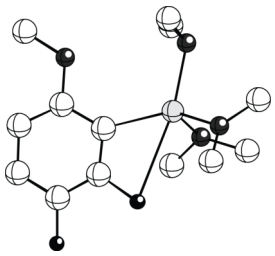

XLVIII

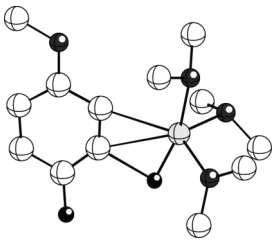

S

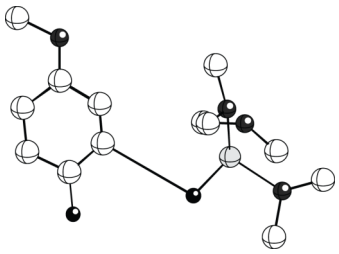

T

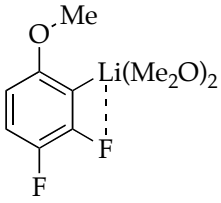

LI

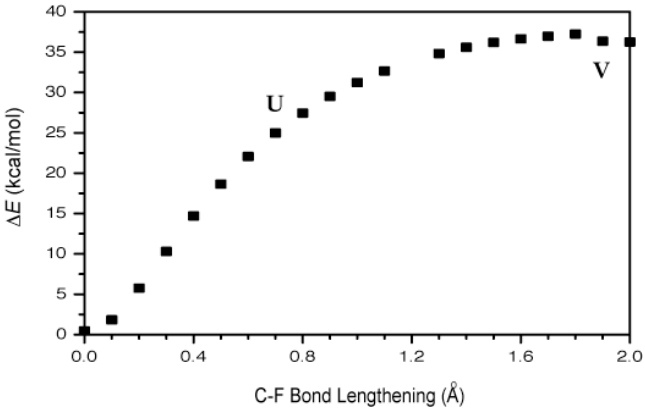

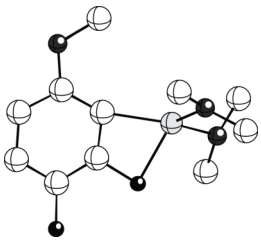

LI

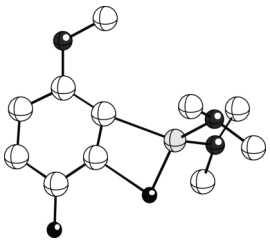

U

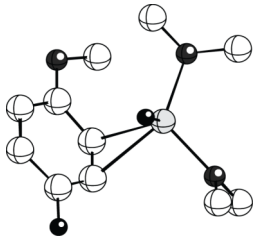

V

XXXIX Experimental Section.

NMR Spectroscopic Analyses. Samples for spectroscopic analyses were prepared by using a protocol described elsewhere [Romesberg, F. E.; Bernstein, M. P.; Fuller, D. J.; Harrison, A. T.; Collum, D. B. *J. Am. Chem. Soc.* **1993**, *115*, 3475]. ^{6}Li and ^{13}C NMR spectra were recorded on a Varian XL-400 spectrometer operating at 58.84 and 100.58 MHz, respectively. The ^{6}Li and ^{13}C resonances are referenced to 0.30 M [^{6}Li]LiCl/MeOH (0.0 ppm, -100 °C), and the THF β-methylene resonance (25.37 ppm, -100 °C), respectively.

Kinetics. For a kinetic run corresponding to a single rate constant, a relatively concentrated (2.2 M) solution of *n*-BuLi in pentane at -78 °C was prepared and titrated to determine the precise concentration.[39] The solution was diluted to a concentration appropriate for the particular series and titrated a second time. A series of oven-dried, argon-flushed 5 mL serum vials (8-10 per rate constant) fitted with stir bars were charged with a stock solution containing the haloarene, spiro[2.4]hepta-4,6-diene, THF, and *n*-octane as a GC standard. The reaction vials were held under argon at –25.0 $\pm$ 0.2 °C (–50.0 $\pm$ 0.5 °C for the 3,4-dihaloanisoles). The reactions were initiated by adding aliquots of a stock solution of *n*-BuLi in hydrocarbon, also refrigerated, to achieve a concentration 0.1 M below the actual haloarene concentration. The vessels were periodically quenched with 1:1 H_2O-THF at intervals chosen to ensure an adequate sampling of early conversion at 10% consumption of the starting material. The quenched aliquots were extracted into pentane and the extracts analyzed using an auto injecting GC fitted with a 30 meter HP-5 column. The metalations were monitored by following the decrease of haloarene relative to the internal standard. The initial rates were determined by least-squares analyses, and were shown to be reproducible within $\pm$ 10%. Following the formation of the corresponding cycloadducts **5** afforded equivalent rates within $\pm$ 10%. The observed rate constants (k_{obsd}) were calculated by dividing the initial rates (linear slopes) by the corresponding concentrations of haloarene. The reported errors correspond to one standard deviation.

XL. Physical and Spectral Data.

5-Chloro-9,9-spirocyclopropyl-1,4-dihydro-1,4-methano-naphthalene (5a).

Clear colorless oil. TLC: $R_f = 0.60$ (100% hexanes); MS m/z 202 $(M)^+$. ^1H NMR (400 MHz, $CDCl_3$) δ 7.04 (d, $J = 6.6$ Hz, 1H), 6.89 (dd, $J = 7.9$, 1.2 Hz, 1H), 6.87-6.82 (m, 3H), 3.56 (d, $J = 2.1$ Hz, 1H), 3.32 (br s, 1H), 0.67-0.52 (m, 2H), 0.50-0.43 (m, 2H); Anal. Calcd for $C_{13}H_{11}Cl$: C, 77.04; H, 5.47. Found: C, 75.78; H, 5.57. Anal. Calcd for $C_{13}H_{11}Cl \cdot 1/4H_2O$: C, 75.36; H, 5.59.

5-Fluoro-9,9-spirocyclopropyl-1,4-dihydro-1,4-methano-naphthalene (5b).

Clear colorless oil. TLC: $R_f = 0.60$ (100% hexanes); MS m/z 186, 184 $(M)^+$. ^1H NMR (400 MHz, $CDCl_3$) δ 6.97 (d, $J = 7.0$ Hz, 1H), 6.87 (m, 1H), 6.83 (br s, 2H), 6.63 (ddd, $J = 8.7$, 8.3, 0.9 Hz, 1H), 3.58 (d, $J = 1.6$ Hz, 1H), 3.32 (m, 1H), 0.66-0.61 (m, 2H), 0.60-0.45 (m, 2H); Anal. Calcd for $C_{13}H_{11}F$: C, 83.84; H, 5.95. Found: C, 83.40; H, 6.12.

5-Chloro-8-methoxy-9,9-spirocyclopropyl-1,4-dihydro-1,4-methano-naphthalene (5c). White solid. TLC: $R_f = 0.30$ (5% diethyl ether in hexanes). ^1H NMR (500 MHz, $CDCl_3$): δ 6.92-6.87 (m, 3H), 6.52 (d, $J = 8.9$ Hz, 1H), 3.79 (s, 3H), 3.62 (m, 1H), 3.58 (m, 1H), 0.68-0.63 (m, 2H), 0.56-0.51 (m, 2H). ^{13}C NMR (125 MHz, $CDCl_3$): δ 152.2, 151.4, 142.8, 142.0, 140.4, 125.7, 120.2, 110.6, 65.9, 56.2, 55.1, 53.0, 9.6, 9.1.

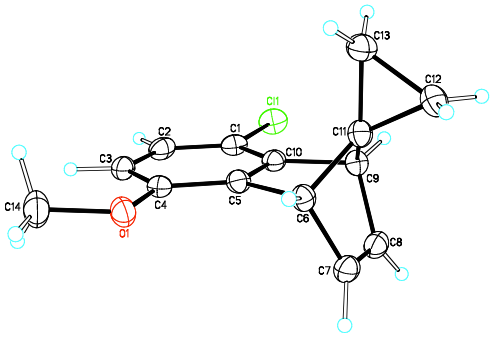

5-Fluoro-8-methoxy-9,9-spirocyclopropyl-1,4-dihydro-1,4-methano-naphthalene (5d). White solid. TLC: $R_f = 0.30$ (5% diethyl ether in hexanes). ^{1}H NMR (500 MHz, $CDCl_3$): δ 6.90-6.88 (m, 2H), 6.65-6.62 (m, 1H), 6.53-6.50 (m, 1H), 3.79 (s, 3H), 3.61 (m, 2H), 0.66-0.64 (m, 2H), 0.55-0.52 (m, 2H). ^{13}C NMR (125 MHz, $CDCl_3$): δ 153.3, 150.7 (d, J = 177 Hz), 142.6, 142.2, 141.2 (d, J = 5 Hz), 138.2 (d, J = 22 Hz), 112.9 (d, J = 24 Hz), 110.4 (d, J = 7 Hz), 66.1, 56.6, 52.6, 52.3, 9.6, 9.1.